TOXICOLOGICAL SCIENCES **119(1)**, 189–208 (2011)
doi:10.1093/toxsci/kfq314
Advance Access publication October 20, 2010

In Utero and Lactational Exposure to a Complex Mixture of Polychlorinated Biphenyls: Toxicity in Pups Dependent on the *Cyp1a2* and *Ahr* Genotypes

Christine P. Curran,*[,1] Charles V. Vorhees,† Michael T. Williams,† Mary Beth Genter,* Marian L. Miller,* and Daniel W. Nebert*[,2]

*Department of Environmental Health and Center for Environmental Genetics, University of Cincinnati Medical Center, Cincinnati, Ohio 45267-0056; and †Department of Pediatrics, Division of Neurology, University of Cincinnati Medical Center, and Cincinnati Children's Research Foundation, Cincinnati, Ohio 45229

[1]Present address: Department of Biological Sciences, Northern Kentucky University, Highland Heights, KY 41099.
[2]To whom correspondence should be addressed. Fax: (513) 821-4664. E-mail: dan.nebert@uc.edu.

Received August 5, 2010; accepted October 7, 2010

Polychlorinated biphenyls (PCBs) are persistent toxic pollutants occurring as complex mixtures in the environment. Humans are known genetically to have > 60-fold differences in hepatic cytochrome P450 1A2 (CYP1A2) levels and > 12-fold differences in aryl hydrocarbon receptor (AHR) affinity, both of which could affect PCB pharmacokinetics. Thus, we compared *Ahr^{b1}_Cyp1a2(+/+)* high-affinity AHR wild-type, *Ahr^{d}_Cyp1a2(+/+)* poor affinity AHR wild-type, *Ahr^{b1}_Cyp1a2(−/−)* knockout, and *Ahr^{d}_Cyp1a2(−/−)* knockout mouse lines. We chose a mixture of three coplanar and five noncoplanar PCBs to reproduce that seen in human tissues, breast milk, and the food supply. The mixture was given by gavage to the mother on gestational day 10.5 (GD10.5) and postnatal day 5 (PND5); tissues were collected from pups and mothers at GD11.5, GD18.5, PND6, PND13, and PND28. *Ahr^{b1}_Cyp1a2(−/−)* pups showed lower weight at birth and slower rate of growth postnatally. Absence of CYP1A2 resulted in significant splenic atrophy at PND13 and PND28. Presence of high-affinity AHR enhanced thymic atrophy and liver hypertrophy in the pups. Concentrations of each congener were analyzed at all time points: maximal noncoplanar congener levels in maternal tissues were observed from GD18 until PND6, whereas the highest levels in pups were found between PND6 and PND28. Coplanar PCB concentrations were generally higher in *Ahr^{d}*-containing pup tissues; these findings are consistent with earlier studies demonstrating the crucial importance of AHR-mediated inducible CYP1 in the gastrointestinal tract as a means of detoxication of oral planar polycyclic aromatic hydrocarbons.

Key Words: **PCB congeners; PCB mixture; *in utero* exposure; immunosuppression; gas chromatography/electron capture detection; cytochrome P450 1A2; aryl hydrocarbon receptor; developmental toxicity.**

Polychlorinated biphenyl (PCB) production was banned worldwide between 1977 and 1984; yet, environmental contamination remains a serious problem. Human populations show striking accumulations of PCBs, with reported levels of > 1700 ng/g lipid in human breast milk samples (WHO, 1996) and 3105 ng/g of lipid in serum from residents residing near highly contaminated sites (Petrik *et al.*, 2006). Major sources of human exposure include placental transfer and ingestion of contaminated food—especially breast milk and fatty fish (ATSDR, 2001).

Out of 209 possible PCB congeners, our present study included a mixture of eight (Fig. 1). Congeners having chlorine atoms only in ortho positions are noncoplanar because of steric hindrance, whereas those with chlorines only in meta and/or para positions are coplanar. Coplanar PCBs are potent ligands for aryl hydrocarbon receptor (AHR) (Poland and Glover, 1977).

Acute PCB exposure can cause chloracne, darkened skin and nail pigmentation, hearing loss, eye disorders, jaundice (Guo *et al.*, 1999), and various neurological symptoms (Masuda, 2001). Chronic low-level PCB exposure—because of industrial pollution or consumption of contaminated food (Schantz *et al.*, 1996)—can increase risk of immunosuppression (Gustavsson and Hogstedt, 1997), cardiovascular disease (Gustavsson and Hogstedt, 1997), and cancer (Negri *et al.*, 2003). Chronic PCB exposure also can disrupt glucose metabolism (Imbeault *et al.*, 2002), thyroid hormone signaling (Tan and Zoeller, 2007), and estrogen and testosterone signaling (Battershill, 1994). Most of these effects appear to be mediated via AHR (Simon *et al.*, 2007).

AHR, when activated by ligand, can up- and downregulate hundreds of genes (Sartor *et al.*, 2009), including increased expression of the three mouse *Cyp1* genes. The prototypical AHR agonist is 2,3,7,8 tetrachlorodibenzo-*p*-dioxin (TCDD; "dioxin"). Other exogenous planar AHR ligands include benzo[*a*]pyrene (BaP), other polycyclic hydrocarbons (PAHs), and coplanar polyhalogenated biphenyls (Nebert, 1989). Toxic equivalency factors (TEFs) are used to estimate a chemical's

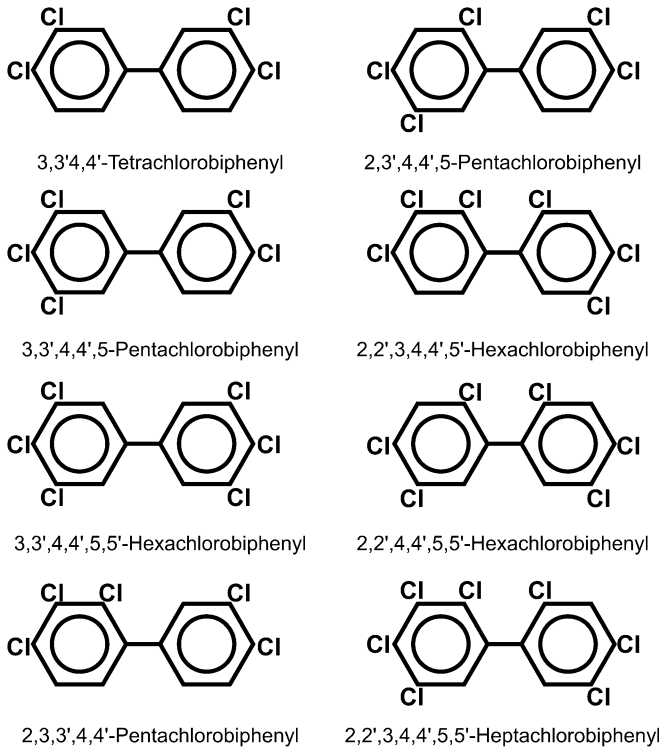

FIG. 1 Chemical structures of the eight PCBs used in this study. Meta- and para-substituted congeners (first three in left row) are coplanar molecules and are able to bind AHR. The remaining five are ortho-substituted congeners and are noncoplanar.

TABLE 1
List of PCB Congeners in the Mixture Used in This Study

PCB congener	Planarity	IUPAC #	Dose/kg	TEF[a]
3,3′4,4′ -Tetrachlorobiphenyl	Coplanar	77	5 mg	0.0005
3,3′,4,4′,5 -Pentachlorobiphenyl	Coplanar	126	25 μg	0.1
3,3′,4,4′,5,5′ -Hexachlorobiphenyl	Coplanar	169	250 μg	0.03
2,3,3′,4,4′ -Pentachlorobiphenyl	Noncoplanar	105	10 mg	0.00003
2,3′,4,4′,5 -Pentachlorobiphenyl	Noncoplanar	118	10 mg	0.00003
2,2′,3,4,4′,5′ -Hexachlorobiphenyl	Noncoplanar	138	10 mg	0.0005
2,2′,4,4′,5,5′ -Hexachlorobiphenyl	Noncoplanar	153	10 mg	0.0005
2,2′,3,4,4′,5,5′ -Heptachlorobiphenyl	Noncoplanar	180	10 mg	0.00001

Note. IUPAC, International Union of Pure and Applied Chemistry.
[a]Listed in Van den Berg *et al.* (2006).

toxicity based on several factors including its AHR-binding affinity; the TEF for the most potent ligand, TCDD, is set at 1.0 (Bhavsar *et al*., 2007; Van den Berg *et al*., 2006).

AHR allelic differences have been reported. In mice, a single amino acid change accounts for much of the 15- to 20-fold differences in affinity (Poland *et al*., 1994); the C57BL/6J (B6) Ahr^{b1} allele encodes the high-affinity AHR and the DBA/2J (D2) Ahr^{d} allele the poor affinity AHR (Nebert *et al*., 2000). In humans, there is a > 12-fold difference in TCDD binding to AHR, although DNA sequences responsible have not yet been identified (Nebert *et al*., 2004).

In utero exposure of laboratory animals to dioxin-like compounds, including coplanar PCBs, can result in birth defects—such as cleft palate and hydronephrosis—and immunosuppression (Selgrade, 2007). In a comparison of B6 mice and the congenic B6.D2-Ahr^{d} line treated *in utero* with polybrominated biphenyls, B6 mice are at ~20-fold greater risk than B6.D2-Ahr^{d} mice for neonatal lethality (Curran *et al*., 2006).

Cytochrome P450 1A2 (CYP1A2) is one of three members of the mammalian CYP1 family (Nelson *et al*., 2004). This enzyme metabolizes estrogen, uroporphyrinogen, and melatonin; CYP1A2 also metabolizes environmental arylamines, as well as about two dozen drugs including caffeine, theophylline, and acetaminophen (Nebert *et al*., 2004).

In human populations, there is > 60-fold variation in hepatic CYP1A2 basal and inducible levels (Nebert *et al*., 2004); yet, no DNA sequence within or near the *CYP1A2* gene unequivocally responsible for this trait has been found (Jiang *et al*., 2006). Intriguingly, the CYP1A2 protein is also able to sequester planar AHR ligands (Hakk *et al*., 2009). The

TABLE 2
Genotypes of Mice Chosen for These Studies

AHR allele	AHR ligand affinity	CYP1A2	Genotype	Common name	Predicted phenotype[a]
Ahr^{b1}	High affinity	Absent	$Ahr^{b1}Cyp1a2(-/-)$	*Cyp1a2(−/−)* knockout	Most vulnerable to PCB mixture
Ahr^{d}	Poor affinity	Absent	$Ahr^{d}Cyp1a2(-/-)$		Almost as vulnerable
Ahr^{d}	Poor affinity	Present	$Ahr^{d}Cyp1a2(+/+)$	B6.D2-Ahr^{d}	Almost as resistant
Ahr^{b1}	High affinity	Present	$Ahr^{b1}Cyp1a2(+/+)$	C57BL/6J (B6)	Most resistant

[a]We predict that the most important factor—leading to PCB-induced poor growth rate—would be absence of maternal liver CYP1A2. Of less importance, but still to be reckoned with, is the high-affinity AHR maternal-fetal unit in which CYP1 enzymes are highly induced by the coplanar PCB ligands (and therefore PCBs are cleared from the tissues); alternatively, and competing with detoxication, more reactive PCB intermediates might be formed.

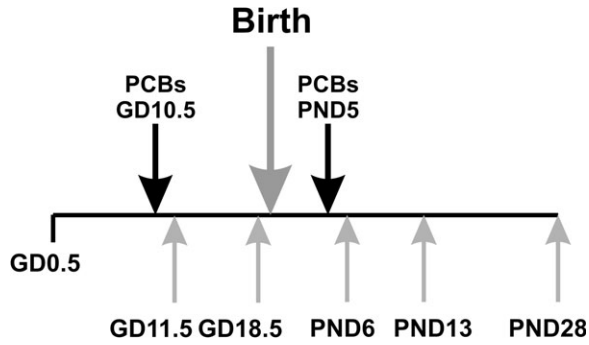

FIG. 2 Experimental time line. The time line shows when mothers were treated and when tissues were collected. Note that the mother was gavaged a second time on PND5, so that the only source of PCBs to the pups would be via lactation.

protective role of maternal mouse hepatic CYP1A2 was directly demonstrated—by comparing *Cyp1a2(+/+)* wild-type with *Cyp1a2(−/−)* knockout pregnant mice treated *in utero* with TCDD; replacement of the mouse *Cyp1a2* gene with the human *CYP1A2* gene evoked the same protective effect (Dragin *et al*., 2006). When the CYP1A2 enzyme is absent, offspring are approximately sixfold more sensitive to dioxin-induced cleft palate, hydronephrosis, and embryolethality compared with *Cyp1a2(+/+)* mice; greater amounts of TCDD were shown to reach *Cyp1a2(−/−)* fetuses, thereby making them more susceptible to teratogenesis (Dragin *et al*., 2006).

In our present study, we chose to compare high-affinity Ahr^{b1} with poor affinity Ahr^{d} mice combined with presence or absence of the *Cyp1a2* gene; this would simulate the extremes of *AHR* and *CYP1A2* gene expression in human populations. Rather than a single congener, we administered an environmentally relevant PCB mixture—one that mirrors levels of various congeners found in human tissues, breast milk, and the food supply. Lastly, we wished to give PCBs at appropriate developmental ages and at sufficiently low concentrations so as not to cause substantial mortality or overt birth defects, yet high enough to ensure that differences in behavioral phenotype might be seen when the offspring reach adulthood. This report describes an analysis of the concentrations of various PCB congeners in several tissues *in utero*, postnatally and in the mother, as well as toxic effects observed. A subsequent report (Curran, Genter, Patel, Vorhees, Williams, and Nebert, in preparation) will describe the behavioral studies.

MATERIALS AND METHODS

Chemicals. All PCB congeners (Table 1, Fig. 1) were purchased from ULTRA Scientific (North Kingstown, RI). The PCBs were dissolved in acetone (5 mg/ml), and the resulting solutions were dissolved in corn oil; the acetone was removed under a gentle stream of argon during magnetic stirring. All other chemicals and reagents were bought from either Fisher Chemical (Fairlawn, NJ) or Sigma Chemical Company (St Louis, MO) as the highest available grades.

Animals. We used four groups of mice—representing the extremes for AHR affinity and CYP1A2 expression in human populations (Table 2). C57BL/6J (B6) and B6.D2-Ahr^{d} (congenic line having DBA/2J poor affinity Ahr^{d} allele on B6 background) mice were purchased from The Jackson Laboratory (Bar Harbor, ME); both are *Cyp1a2(+/+)* wild type. The Ahr^{b1}*_Cyp1a2(−/−)* knockout mouse line was created by the Nebert laboratory (Liang *et al*., 1996). A novel Ahr^{d}*_Cyp1a2(−/−)* line was developed by mating *Cyp1a2(−/−)* mice with the B6.D2-Ahr^{d} line. By means of at least eight backcrosses into B6 mice, all four genotypes are expressed in a > 99.8% B6 genetic background, which should reduce experimental noise. Animals were housed in the University of Cincinnati's Laboratory Animal Medicine Facilities, having a 12:12-h light-dark cycle. Standard care included rodent chow (Lab Diet 5001; Purina Mills, Richmond, IN) and water *ad libitum* with pregnant mothers receiving breeder chow (Lab Diet 5015; Purina Mills) from gestational day 0.5 (GD0.5) through weaning. All mouse experiments were conducted in accordance with the National Institutes of Health standards for the care and use of experimental animals and the University of Cincinnati's Medical Center Institutional Animal Care and Use Committee.

Breeding protocol. Nulliparous females 3–5 months of age (20–25 g) were used for all matings. The morning when a vaginal plug was found was considered GD0.5; plug-positive females were removed from the breeding cage. Pregnant females were housed individually with pups until weaning on postnatal day 28 (PND28).

Dosing of animals. Pregnant females were given PCBs by gavage on GD10.5 and a second time on PND5 (Fig. 2); this time point was chosen to insure continual AHR activation throughout lactation and was based on our own preliminary data. Control animals received an equivalent volume of corn oil vehicle alone (15 ml/kg). Dosing was delayed until GD10.5 to avoid interfering with embryo implantation and to minimize neonatal lethality (Curran *et al*., 2006). Between GD10.5 and PND20 (gestation plus lactation) comprises the period of rodent brain development that most closely matches brain development in the second to early third trimesters of human development (Clancy *et al*., 2007). Another manuscript will describe neurobehavioral studies in these mice, tested between days PND60 and PND100 (Curran, Genter, Patel, Vorhees, Williams, and Nebert, in preparation).

TABLE 3
Primers Used in These Studies

Gene	Forward primer	Reverse primer
Cyp1a1	5′-CAGACCTCAGCTGCCCTATC-3′	5′-CTTGCCCAAACCAAAGAGAG-3′
Cyp1a2	5′-ACAACGAGGGACACCTCAC-3′	5′-GGGATCTCCCCAATGCAC-3′
Actb	5′-CATCCGTAAAGACCTCTATGCC-3′	5′-ACGCAGCTCAGTAACAGTCC-3′

Note. The probes for the mouse *Cyp1a1* and *Cyp1a2* genes detect CYP1A1 and CYP1A2 mRNA, respectively. The probe for the mouse β-actin (*Actb*) gene detects ACTB mRNA.

TABLE 4
Assessment of Birth Weights and Neonatal Lethality

Genotype	Treatment	Birth weight (g)	Dystocia cases (% pregnancies)	Abnormal gestation (% pregnancies)[a]	Litter size	Neonatal lethality (%)
Ahr^{b1}_Cyp1a2(+/+)	Corn oil	1.33 ± 0.01	0	5.9	7.8 ± 0.3	6.8
Ahr^{b1}_Cyp1a2(+/+)	PCB	1.32 ± 0.01	18	5.3	8.3 ± 0.5	15
Ahr^{d}_Cyp1a2(+/+)	Corn oil	1.32 ± 0.01	6.7	0	8.1 ± 0.3	3.5
Ahr^{d}_Cyp1a2(+/+)	PCB	1.33 ± 0.01	16	0	7.7 ± 0.4	13
Ahr^{b1}_Cyp1a2(−/−)	Corn oil	1.30 ± 0.01	0	0	7.9 ± 0.4	8.7
Ahr^{b1}_Cyp1a2(−/−)	PCB	1.27 ± 0.01*	21	22	7.0 ± 0.4	14
Ahr^{d}_Cyp1a2(−/−)	Corn oil	1.32 ± 0.02	0	0	7.6 ± 0.4	12
Ahr^{d}_Cyp1a2(−/−)	PCB	1.28 ± 0.01*	26	21	8.0 ± 0.4	21

Note. All values are expressed as means ± SEM.
[a]Abnormal gestation refers to pregnancies that ended prematurely or were prolonged beyond the normal 19.5-day gestational length.
*Significantly different from all other groups. $p < 0.001$; N was ≥ 10 litters per group.

Plasma total thyroxine assay. T4 levels were measured using a standard enzyme immunoassay kit (ALPCO Diagnostics, Salem, NH) following the manufacturer's protocol. Blood was collected in heparinized tubes following decapitation and centrifuged at 2500 × g for 5 min at 4°C, and the plasma fraction was stored at −80°C until analysis. Samples were collected from GD18.5 fetuses (pooled from 2 to 3 fetuses per sample) and pups at PND6, PND13, and PND28 (1 pup per sample). All samples were run in duplicate. T4 levels were calculated by comparison with a standard curve.

Gas chromatography with electron capture detection. Gas chromatography with electron capture detection (GC-ECD) was used to analyze the concentration of individual PCB congeners. Figure 2 shows a time line of treatment and tissue collection. Using a modification of previously developed methods (Imsilp *et al.*, 2005), it was possible to detect all eight congeners included in the dosing mixture. Samples from control tissues were analyzed, and we found no interfering peaks or quantifiable PCB levels.

Tissues were collected following carbon dioxide asphyxiation, rinsed in ice-cold 1× PBS, blotted, snap frozen on dry ice, and stored at −80°C until processing. Tissues were collected at GD11.5, GD18.5, PND6, PND13, and PND28 time points. Tissues included the following: maternal brain, liver, mammary gland, and adipose tissue from the inguinal fat pad; pup brain, liver, subcutaneous fat, stomach contents, adipose tissue from the inguinal fat pad; and plasma. At GD11.5, two whole embryos were pooled for analysis. At GD18.5, brain (pooled from two fetuses) and liver (from a single fetus) were analyzed. Adipose samples from PND6 litters, as well as PND13 litters, were pooled, using both subcutaneous fat and inguinal fat pad. At PND28, there was sufficient adipose tissue available to analyze subcutaneous fat and the inguinal fat pad separately.

Tissue samples were weighed and homogenized in 2.5 ml of a 1:1 (vol/vol) solution of analytical grade hexane and acetone. PCB 65 (2,3,5,6-tetrachlorobiphenyl) was used as an internal standard with 25 µl of a 2 µg/ml solution (50 ng total) added to each sample prior to homogenization. Homogenates were centrifuged for 5 min at 2500 × g and the supernatant fractions collected; the extraction procedure was repeated three times. Tissue (~150 mg) or plasma (~100 µl) was used for each sample. Supernatant fractions were pooled and filtered using a solvent-resistant 0.45-µm polyvinylidene fluoride filter (Millipore; Burlington, MA). The filter was rinsed once with 1 ml hexane. Water was removed from the pooled supernatants using anhydrous sodium sulfate. Samples were then dried to dampness under a gentle stream of argon in a 40°C water bath. All sample preparation was done using glass tubes, pipettes, and syringes.

Samples were reconstituted in 1 ml analytical grade hexane, and 1 µl was injected into an Agilent 6890N gas chromatography system using a 60-m × 0.25-mm × 0.25-µm DB-5 capillary column and a microelectron capture detector. The carrier gas was helium, and the makeup gas was argon-methane (95:5%). Injector and detector temperatures were 250°C and 325°C, respectively. The column oven was programmed to increase from

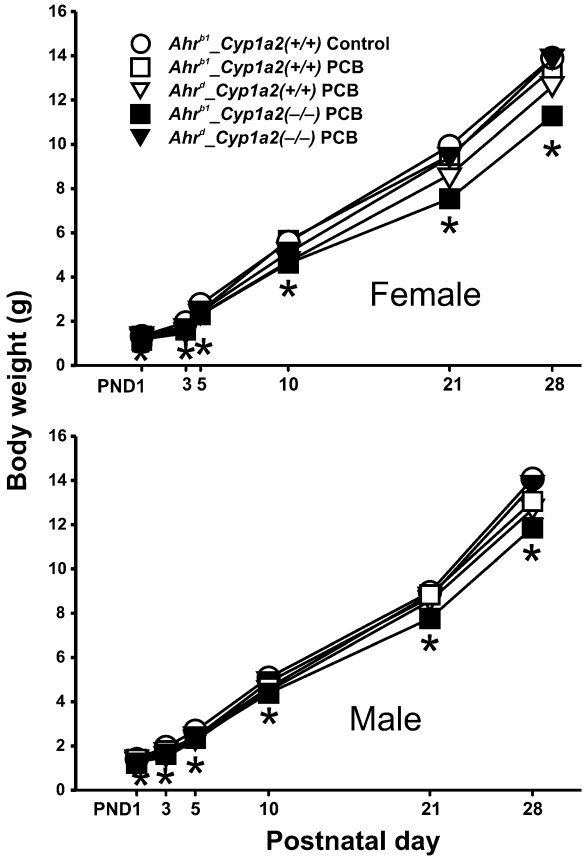

FIG. 3 Body weights from PND1 through PND28. (A) Females. (B) Males. PCB treatment always appeared to decrease growth rates slightly throughout the lactational period. Data are presented as mean values ± SEM. $N \geq 10$ per time point. *p Value < 0.001.

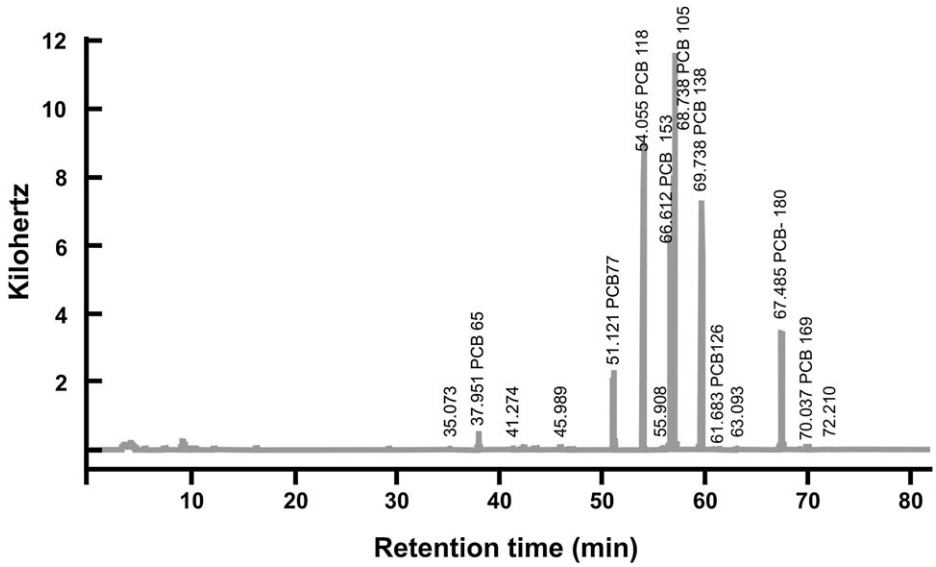

FIG. 4 GC-ECD sample chromatogram. GC-ECD was used to quantify PCB congeners. Depicted is a sample chromatogram showing the results from adipose tissue taken from an *Ahr*^{b}*_Cyp1a2(−/−)* mother at GD11.5; a software program was used to identify and quantify each of the eight congeners.

145°C to 275°C at 1.5°C per min and then increased to 300°C at 8°C per min, holding at 300°C for 5 min. The injector was operated in the split/splitless mode.

Data were collected and analyzed using ChemStation software (Hewlett Packard/Agilent Technologies, Wilmington, DE). Calibration standards of 5–200 ng/ml, spiked with 50 ng of internal standard, were used to construct calibration curves. All standard curves had correlations with $R^2 \geq 0.998$. Limits of quantification were 0.5 ng/100 mg and 0.5 ng/100 µl of tissue and plasma, respectively. The interassay coefficient of variance was less than 4%, and check standards were run daily.

Total RNA preparation and reverse transcription. Mice were euthanized using carbon dioxide asphyxiation followed by decapitation for tissue collection at two prenatal and three postnatal time points (Fig. 2). Tissues were rinsed in ice-cold 1× PBS, blotted, snap frozen on dry ice, and stored at −80°C until processing. Total RNA was isolated from liver, brain, and whole embryos (GD11.5)—homogenized in 1 ml/100 mg TriReagent (Molecular Research Corporation, Inc., Cincinnati, OH)—and RNA was extracted using the manufacturer's protocol. The cDNA was synthesized using reverse-iT (AbGene) and the replacement Verso kits (Thermo Scientific; Waltham, MA), oligo-dT primers, and 2 µg total RNA. The manufacturer's 2-step protocol was used for all samples.

Quantitative real-time PCR. We carried out quantitative real-time PCR (qRT-PCR) using a DNA Engine Opticon-2 Real-Time PCR Detection System (MJ Research). Samples were prepared in 20-µl volume reactions with 1 µg cDNA added to 7 µl water, 1 µl of each primer (10µM solutions), and 10 µl iQ SYBR Green Supermix (Bio-Rad Laboratories, Hercules, CA) for each sample. Table 3 shows the primer sets used.

All primers were designed to cross at least two exons to avoid confounding by any contaminating genomic DNA. The "housekeeping genes" glyceraldehyde-3-phosphate dehydrogenase and β-actin (ACTB) messenger RNA (mRNAs) were both scrutinized to be sure that they were not affected by PCB treatment; subsequently, ACTB was chosen as the preferred internal standard. Results were normalized to ACTB expression for both liver and brain. Values were expressed as the CYP1A1 or CYP1A2 mRNA/ACTB mRNA ratios over corn oil–treated controls using control animals of the same age. $N = 3$–5 per group. Quantification of fold changes was done using the delta-delta C_t method (Karlen *et al.*, 2007). The primer sets for target genes and the control gene were tested and, in our hands, found to have similar PCR efficiency (± 3%)—both of which were close to 100% efficiency, as determined originally by curves of standards. Hence, we were able to use the delta-delta C_t method without needing to generate standard curves each time. PCR products run on a 2% agarose gel confirmed a single band of the appropriate size.

Histology. Animals were perfused transcardially with 4% paraformaldehyde and small sections of liver and brain removed and soaked overnight in the same preservative. Slices (4 µm) of paraffin-embedded tissue were rehydrated, stained with hematoxylin and eosin, and visualized by light microscopy.

Chemical hazard precaution. PCBs are not only very toxic but also some are likely human carcinogens. All personnel were instructed in safe handling procedures. Laboratory coats, gloves, and masks were worn at all times, and contaminated materials were collected separately for disposal by the Hazardous Waste Unit or by independent contractors. PCB-fed mice were housed separately, and their carcasses treated as contaminated biological materials.

Statistical analysis. SigmaPlot 9.0 and SigmaStat 3.1 (Systat Software Inc.; San Jose, CA) were used for statistical analysis of litter size and pup weights, using two-way ANOVAs to consider the factors of genotype and treatment and their interaction. Many comparisons included all treated groups versus control *Ahr*^{b1}*_Cyp1a2(+/+)* mice, which were one-way ANOVAs, followed by Holm-Sidak multiple pairwise comparisons. Data are presented as means ± SEM. p Values of < 0.05 were regarded as statistically significant for all comparisons.

RESULTS

Selection of PCB Congeners for This Study

Rather than a single congener, we wished to study an environmentally relevant mixture of PCBs—one that most closely mimicked human exposures. The congeners selected represent those having been identified as among the most toxic and most prevalent by the World Health Organization (Van den Berg *et al.*, 2006) and those that are commonly found in the

TABLE 5
Coplanar PCB Congener Analysis on GD11.5

Genotype	Tissue	PCB 77	PCB 126	PCB 169
Ahr^{b1}Cyp1a2(+/+)	Maternal brain	< 0.5	< 0.5	< 0.5
Ahr^{d}Cyp1a2(+/+)		12.8 ± 2.0	< 0.5	< 0.5
Ahr^{b1}Cyp1a2(−/−)		2.7 ± 0.4	< 0.5	< 0.5
Ahr^{d}Cyp1a2(−/−)		17.0 ± 1.8	< 0.5	< 0.5
Ahr^{b1}Cyp1a2(+/+)	Maternal liver	28.3 ± 2.7	3.6 ± 1.6	25.2 ± 6.5
Ahr^{d}Cyp1a2(+/+)		93.5 ± 12	1.8 ± 0.4	9.9 ± 1.6
Ahr^{b1}Cyp1a2(−/−)		15.2 ± 2.0	1.8 ± 0.4	10.3 ± 1.2
Ahr^{d}Cyp1a2(−/−)		109 ± 8.5	2.3 ± 0.7	13.7 ± 1.7
Ahr^{b1}Cyp1a2(+/+)	Maternal inguinal fat pad	96.7 ± 10	< 0.5	7.0 ± 1.1
Ahr^{d}Cyp1a2(+/+)		262 ± 18	1.8 ± 0.4	11.8 ± 1.2
Ahr^{b1}Cyp1a2(−/−)		156 ± 9.2	2.2 ± 0.7	13.2 ± 2.7
Ahr^{d}Cyp1a2(−/−)		284 ± 4.1	1.7 ± 0.9	13.7 ± 2.1
Ahr^{b1}Cyp1a2(+/+)	Maternal mammary tissue	96.4 ± 9.7	< 0.5	8.8 ± 1.2
Ahr^{d}Cyp1a2(+/+)		297 ± 43	2.6 ± 0.4	15.2 ± 3.1
Ahr^{b1}Cyp1a2(−/−)		127 ± 4.6	2.0 ± 0.6	11.5 ± 2.1
Ahr^{d}Cyp1a2(−/−)		289 ± 7.7	2.4 ± 0.5	16.2 ± 0.9
Ahr^{b1}Cyp1a2(+/+)	Placenta	< 0.5	< 0.5	< 0.5
Ahr^{d}Cyp1a2(+/+)		5.3 ± 2.8	< 0.5	< 0.5
Ahr^{b1}Cyp1a2(−/−)		5.3 ± 1.8	< 0.5	< 0.5
Ahr^{d}Cyp1a2(−/−)		15.3 ± 1.2	< 0.5	< 0.5
Ahr^{b1}Cyp1a2(+/+)	Whole embryo[a]	< 0.5	< 0.5	< 0.5
Ahr^{d}Cyp1a2(+/+)		6.3 ± 1.1	< 0.5	< 0.5
Ahr^{b1}Cyp1a2(−/−)		4.4 ± 3.2	< 0.5	< 0.5
Ahr^{d}Cyp1a2(−/−)		7.7 ± 0.5	< 0.5	< 0.5

Note. For all 10 tables (Tables 5–14), congeners are ranked according to their planarity and chlorination patterns, with PCB 77 being a coplanar tetrachlorobiphenyl and PCB 180 a noncoplanar heptachlorobiphenyl. All values denote the means of three to five per group ± SEM and represent nanograms per 100 mg tissue wet weight. Limits of quantification were 0.5 ng/100 mg or 0.5 ng/100 µl of tissue or plasma, respectively. For all intergenotype, intercongener, and group comparisons, p values are available upon request. For GD11.5 collection, these tissues were collected 24 h after the initial PCB dose.

[a]Whole embryo represents $N = 2$–3, and two to three placentas were pooled from each mother.

human food supply (Costabeber *et al*., 2006; Dewailly *et al*., 1999) and in human tissues collected during cohort studies (Soechitram *et al*., 2004). We also included the noncoplanar congener PCBs 105 and 118 because they can be metabolized to the neurotoxic metabolite 4-hydroxy-PCB 107 (Meerts *et al*., 2004).

The chemical structures and dosages of all eight congeners, along with their established TEFs, are listed in Table 1 and illustrated in Figure 1. Preliminary studies were conducted using the individual congeners in order to determine a dosing regimen that (1) resulted in AHR-mediated CYP1A1 upregulation through late gestation until weaning in high-affinity AHR (*Ahr^{b1}*) mice and (2) did not cause excessive neonatal lethality (defined as not more than 25% greater lethality than control litters) or teratogenesis. From these preliminary results, the final composition for the mixture of coplanar plus noncoplanar PCBs was ultimately established.

Selection of Genotypes Used in This Study

We wished to have the full range of AHR affinity and levels of CYP1A2 expression in the maternal-fetal unit. Thus, we chose combinations of two lines having the high-affinity AHR and two having the poor affinity AHR plus two lines having the *Cyp1a2(+/+)* wild-type gene and two having the *Cyp1a2(−/−)* genotype (Table 3). Based on previously published data discussed above, we postulated that the *Cyp1a2(−/−)*-containing maternal-fetal units would be most vulnerable to toxic effects of coplanar PCBs seen in the pups and the *Cyp1a2(+/+)*-containing units most resistant. However, addition of five noncoplanar congeners put a wild card into our ultimately decided upon mixture, and we therefore were not certain what to expect.

Litter Statistics and Neonatal Lethality

There were no significant differences in distribution of gender or litter size across genotype or treatment groups—with means of 7–8 pups per litter. Neonatal lethality rates were higher in PCB-treated litters compared with control litters; the highest rate (20%) was seen in PCB-treated *Ahr^{d}_Cyp1a2(−/−)* mice. Neonatal lethality in PCB-treated *Cyp1a2(−/−)* litters was within an acceptable range: $\geq$ 75% of *Cyp1a2(−/−)* newborns survived birth and ~67% of

TABLE 6
Noncoplanar PCB Congener Analysis on GD11.5

Genotype	Tissue	PCB 105	PCB 118	PCB 138	PCB 153	PCB 180
$Ahr^{b1}Cyp1a2(+/+)$	Maternal brain	14.0 ± 2.5	16.2 ± 2.6	23.2 ± 3.7	16.1 ± 2.1	30.4 ± 2.7
$Ahr^{d}Cyp1a2(+/+)$		27.8 ± 3.5	27.6 ± 3.5	32.3 ± 3.9	30.6 ± 3.1	44.6 ± 4.7
$Ahr^{b1}Cyp1a2(-/-)$		25.4 ± 0.8	25.5 ± 0.4	30.6 ± 0.8	26.0 ± 1.9	41.0 ± 2.0
$Ahr^{d}Cyp1a2(-/-)$		26.7 ± 3.5	28.0 ± 3.1	33.4 ± 4.4	28.3 ± 2.7	46.1 ± 6.7
$Ahr^{b1}Cyp1a2(+/+)$	Maternal liver	150 ± 34	135 ± 17	159 ± 18	125 ± 13	222 ± 34
$Ahr^{d}Cyp1a2(+/+)$		183 ± 28	157 ± 16	184 ± 17	149 ± 16	244 ± 21
$Ahr^{b1}Cyp1a2(-/-)$		150 ± 21	123 ± 9.4	145 ± 11	110 ± 5.9	184 ± 14
$Ahr^{d}Cyp1a2(-/-)$		177 ± 18	154 ± 9.5	176 ± 12	141 ± 11	237 ± 14
$Ahr^{b1}Cyp1a2(+/+)$	Maternal inguinal fat pad	293 ± 41	258 ± 60	214 ± 28	173 ± 21	154 ± 19
$Ahr^{d}Cyp1a2(+/+)$		395 ± 23	358 ± 51	287 ± 18	235 ± 18	206 ± 13
$Ahr^{b1}Cyp1a2(-/-)$		381 ± 47	323 ± 66	267 ± 36	207 ± 25	189 ± 32
$Ahr^{d}Cyp1a2(-/-)$		376 ± 3.0	326 ± 5.3	263 ± 4.1	220 ± 12	194 ± 11
$Ahr^{b1}Cyp1a2(+/+)$	Maternal mammary tissue	339 ± 43	302 ± 38	254 ± 34	203 ± 27	184 ± 27
$Ahr^{d}Cyp1a2(+/+)$		441 ± 60	393 ± 54	332 ± 47	267 ± 38	243 ± 35
$Ahr^{b1}Cyp1a2(-/-)$		323 ± 38	278 ± 33	230 ± 30	180 ± 21	163 ± 25
$Ahr^{d}Cyp1a2(-/-)$		400 ± 6.9	365 ± 6.6	301 ± 7.3	244 ± 6.3	219 ± 11
$Ahr^{b1}Cyp1a2(+/+)$	Placenta	7.62 ± 2.0	8.37 ± 2.3	9.8 ± 3.1	9.06 ± 2.7	15.2 ± 5.4
$Ahr^{d}Cyp1a2(+/+)$		16.7 ± 2.4	18.2 ± 2.4	19.9 ± 3.0	19.2 ± 2.7	29.2 ± 4.6
$Ahr^{b1}Cyp1a2(-/-)$		33.1 ± 8.4	32.8 ± 7.8	33.3 ± 8.1	29.3 ± 7.3	43.2 ± 13
$Ahr^{d}Cyp1a2(-/-)$		23.7 ± 1.3	23.7 ± 2.0	26.3 ± 1.7	24.7 ± 0.2	41.4 ± 1.7
$Ahr^{b1}Cyp1a2(+/+)$	Whole embryo[a]	6.2 ± 0.4	7.3 ± 0.3	8.0 ± 0.8	6.7 ± 0.6	8.5 ± 0.5
$Ahr^{d}Cyp1a2(+/+)$		11.5 ± 2.2	11.5 ± 1.9	11.6 ± 2.0	10.6 ± 1.6	16.2 ± 2.4
$Ahr^{b1}Cyp1a2(-/-)$		17.2 ± 6.2	16.1 ± 5.4	15.1 ± 3.8	12.7 ± 3.4	17.2 ± 2.3
$Ahr^{d}Cyp1a2(-/-)$		10.8 ± 0.8	11.2 ± 0.8	10.7 ± 0.7	9.36 ± 0.6	14.4 ± 0.4

Note. For GD11.5 collection, these tissues were collected 24 h after the initial PCB dose.
[a]Whole embryo represents $N = 2$–3, and two to three placentas were pooled from each mother.

Cyp1a2(−/−) pups survived until weaning compared with 70–77% of *Cyp1a2(+/+)* pups. No cases of hydronephrosis or cleft palate were seen in any of the PCB-treated pups. No further attempt was made to determine the cause of neonatal deaths.

Birth weights were significantly lower for pups born to PCB-treated *Cyp1a2(−/−)* mothers regardless of *Ahr* genotype (Table 4). Treatment and genotype provided the two main effects; there was a treatment × genotype interaction. Although statistically significant ($p < 0.001$), it should be noted that the actual difference in mean birth weights across genotypes and treatment groups was < 70 mg.

Overall, PCB-treated mothers experienced higher rates of dystocia and length of gestation abnormalities compared with corn oil–treated mothers regardless of genotype (Table 4). All PCB-treated groups experienced significantly greater incidences of dystocia (~16 to 26% of all pregnancies) than controls; only *Cyp1a2(−/−)* mothers experienced more abnormalities in the length of gestation (~21 to 22% of pregnancies) regardless of their *Ahr* genotype.

Growth Rates

In utero exposure to the PCB mixture caused a statistically significant decrease in growth rate for Ahr^{b1}*_Cyp1a2(−/−)* pups regardless of sex (Fig. 3). p Values increased from < 0.05 at PND3 to < 0.01 at PND5 and < 0.001 from PND10 through PND28.

Plasma T4 Levels

One of the best characterized effects of *in utero* PCB exposure in human populations is a reduction in circulating thyroid hormones (Takser *et al*., 2005; Wang *et al*., 2005). In rodent studies, this effect is seen—regardless of whether coplanar or noncoplanar congeners are administered (Van Birgelen *et al*., 1995).

There were no significant differences in total plasma T4 at GD18 when levels are normally at their lowest. By PND6, we found that PCB-treated Ahr^{b1}*_Cyp1a2(−/−)* pup's T4 levels were decreased to 80% of that in untreated Ahr^{b1}*_Cyp1a2(+/+)* pups ($p < 0.05$). At PND13 and PND28, there was a trend of PCB-treated Ahr^{b1}*_Cyp1a2(−/−)* pups having lower T4 levels than all other genotypes treated or untreated; however, the comparisons were not statistically significant at the $p < 0.05$ level (data not shown).

Histology

In PND28 animals of all treated versus nontreated genotypes, we looked for PCB-induced changes in liver and

TABLE 7
Coplanar PCB Congener Analysis on GD18.5

Genotype	Tissue	PCB 77	PCB 126	PCB 169
Ahr^{b1}Cyp1a2(+/+)	Maternal brain	< 0.5	< 0.5	< 0.5
Ahr^{d}Cyp1a2(+/+)		4.6 ± 0.9	< 0.5	< 0.5
Ahr^{b1}Cyp1a2(−/−)		< 0.5	< 0.5	< 0.5
Ahr^{d}Cyp1a2(−/−)		26.4 ± 1.8	< 0.5	< 0.5
Ahr^{b1}Cyp1a2(+/+)	Maternal liver	4.3 ± 1.3	18.4 ± 1.5	33.9 ± 2.9
Ahr^{d}Cyp1a2(+/+)		18.2 ± 5.4	2.9 ± 0.8	5.4 ± 1.1
Ahr^{b1}Cyp1a2(−/−)		1.5 ± 0.9	< 0.5	5.1 ± 0.8
Ahr^{d}Cyp1a2(−/−)		69.5 ± 7.9	< 0.5	3.6 ± 0.7
Ahr^{b1}Cyp1a2(+/+)	Maternal inguinal fat pad	34.4 ± 12	2.8 ± 0.7	52.9 ± 7.2
Ahr^{d}Cyp1a2(+/+)		149 ± 29	5.4 ± 1.3	63.1 ± 10.5
Ahr^{b1}Cyp1a2(−/−)		44.3 ± 6.8	8.9 ± 1.0	62.9 ± 8.9
Ahr^{d}Cyp1a2(−/−)		434 ± 19	8.0 ± 0.6	47.9 ± 5.8
Ahr^{b1}Cyp1a2(+/+)	Maternal mammary tissue	15.2 ± 6.9	1.9 ± 0.2	44.1 ± 2.7
Ahr^{d}Cyp1a2(+/+)		95.7 ± 23	3.1 ± 1.1	50.4 ± 9.9
Ahr^{b1}Cyp1a2(−/−)		17.0 ± 5.2	5.9 ± 0.7	44.3 ± 8.1
Ahr^{d}Cyp1a2(−/−)		371 ± 18	6.2 ± 0.5	38.3 ± 4.1
Ahr^{b1}Cyp1a2(+/+)	Fetal brain	< 0.5	< 0.5	< 0.5
Ahr^{d}Cyp1a2(+/+)		2.7 ± 1.0	< 0.5	< 0.5
Ahr^{b1}Cyp1a2(−/−)		< 0.5	< 0.5	< 0.5
Ahr^{d}Cyp1a2(−/−)		18.8 ± 3.1	< 0.5	< 0.5
Ahr^{b1}Cyp1a2(+/+)	Fetal liver	< 0.5	< 0.5	< 0.5
Ahr^{d}Cyp1a2(+/+)		3.59 ± 1.5	< 0.5	< 0.5
Ahr^{b1}Cyp1a2(−/−)		< 0.5	< 0.5	< 0.5
Ahr^{d}Cyp1a2(−/−)		21.3 ± 2.3	< 0.5	< 0.5

Note. These tissues were collected 8 days after the first gavage on GD10.5.

in overall brain structure and development. Using coded samples so that the observer was unaware of the genotype or treatment, histological examination showed no overt changes detectable in either liver or several areas of brain (data not shown).

Detection of PCB Congeners in Tissues of Mother and Pup

Figure 4 depicts a typical GC-ECD chromatogram—enhanced to highlight individual retention times for each PCB congener. Analysis of PCB congeners was carried out on GD11.5, GD18.5, PND6, PND13, and PND28 (Tables 5–14). Several of the coplanar PCBs were below the level of detection in many tissues, whereas all the noncoplanar PCBs were always detected—until PND28. In general, all the coplanar congeners were highest in maternal inguinal fat pad, whereas all the noncoplanar congeners were highest in both maternal inguinal fat pad and mammary tissue. In the postnatal pup, all eight PCBs were highest in adipose tissue.

On GD11.5, 24 h after the first gavage (Tables 5 and 6), all three coplanar congeners were lowest in *Ahr^{b1}_Cyp1a2(+/+)* maternal inguinal fat pad compared with the other three genotypes. On the other hand, all three coplanar congeners were highest in *Ahr^{d}_Cyp1a2(−/−)* maternal mammary tissue compared with the other three genotypes. In placenta and whole embryo, all three coplanar congeners were lowest in *Ahr^{b1}_Cyp1a2(+/+)*. The coplanar PCB 126 and PCB 169 were below the limits of detection in maternal brain, the placenta, and the whole embryo—for all four genotypes. All five noncoplanar congeners were lowest in *Ahr^{b1}_Cyp1a2(+/+)* maternal brain, the placenta, and the whole embryo.

On GD18.5, 8 days after the first gavage (Tables 7 and 8), the coplanar PCB 77 was highest in *Ahr^{d}_Cyp1a2(−/−)* maternal brain, liver, inguinal fat pad and mammary tissue, and fetal brain and liver compared with that in the other three genotypes. Except for PCB 169 levels being considerably higher than PCB 126 levels (because of 10-fold greater PCB 169 concentration in the dosing solution), these two other coplanar congeners were not different among the tissues or genotypes. PCB 126 and PCB 169 were below the limits of detection in maternal and fetal brain and fetal liver—for all four genotypes; these data confirm that the dose given on GD10.5 was beginning to disappear. All five noncoplanar congeners were unremarkable, except for being highest in *Ahr^{b1}_Cyp1a2(+/+)* fetal liver.

On PND6, 24 h after the second gavage (Tables 9 and 10), the coplanar PCB 77 was highest in *Ahr^{d}*-containing mouse lines for all tissues examined: maternal brain, liver, inguinal fat pad, and mammary tissue and pup brain, liver, adipose tissue, and stomach. The other two coplanar congeners, and PCB 126 and PCB 169, were highest in *Ahr^{b1}_Cyp1a2(+/+)* maternal liver and inguinal fat pad compared with that in the other three genotypes. The

TABLE 8
Noncoplanar PCB Congener Analysis on GD18.5

Genotype	Tissue	PCB 105	PCB 118	PCB 138	PCB 153	PCB 180
Ahr^{b1}Cyp1a2(+/+)	Maternal brain	29.4 ± 3.2	30.8 ± 2.5	31.1 ± 2.5	23.1 ± 2.3	32.4 ± 2.4
Ahr^{d}Cyp1a2(+/+)		33.1 ± 2.6	33.2 ± 4.8	30.6 ± 4.8	23.5 ± 3.4	34.4 ± 6.0
Ahr^{b1}Cyp1a2(−/−)		33.4 ± 2.4	32.4 ± 3.3	29.2 ± 2.8	22.5 ± 2.7	32.1 ± 3.6
Ahr^{d}Cyp1a2(−/−)		34.4 ± 2.2	32.6 ± 1.5	30.4 ± 1.6	23.3 ± 1.1	33.0 ± 2.2
Ahr^{b1}Cyp1a2(+/+)	Maternal liver	164 ± 4.5	129 ± 5.0	148 ± 4.0	76.1 ± 21	136 ± 5.5
Ahr^{d}Cyp1a2(+/+)		127 ± 16.7	89.7 ± 13	98.9 ± 16	64.4 ± 10	94.0 ± 16
Ahr^{b1}Cyp1a2(−/−)		145 ± 16	97.5 ± 12	132 ± 14	69.1 ± 10	121 ± 14
Ahr^{d}Cyp1a2(−/−)		126 ± 13	87.9 ± 9.3	109 ± 11	65.4 ± 7.0	107 ± 13
Ahr^{b1}Cyp1a2(+/+)	Maternal inguinal fat pad	639 ± 38	580 ± 38	570 ± 37	448 ± 36	482 ± 34
Ahr^{d}Cyp1a2(+/+)		691 ± 56	614 ± 49	586 ± 51	475 ± 40	515 ± 49
Ahr^{b1}Cyp1a2(−/−)		740 ± 91	657 ± 84	626 ± 79	502 ± 70	541 ± 67
Ahr^{d}Cyp1a2(−/−)		678 ± 43	599 ± 34	559 ± 39	445 ± 29	478 ± 43
Ahr^{b1}Cyp1a2(+/+)	Maternal mammary tissue	514 ± 31	477 ± 31	485 ± 34	386 ± 32	432 ± 38
Ahr^{d}Cyp1a2(+/+)		575 ± 49	516 ± 38	507 ± 44	411 ± 35	486 ± 47
Ahr^{b1}Cyp1a2(−/−)		495 ± 56	449 ± 53	436 ± 53	353 ± 47	412 ± 56
Ahr^{d}Cyp1a2(−/−)		566 ± 42	508 ± 33	496 ± 41	401 ± 31	465 ± 53
Ahr^{b1}Cyp1a2(+/+)	Fetal brain	20.8 ± 1.5	21.5 ± 1.0	21.3 ± 1.1	16.3 ± 1.0	19.8 ± 1.0
Ahr^{d}Cyp1a2(+/+)		18.1 ± 3.3	16.7 ± 3.1	15.3 ± 3.2	12.3 ± 2.6	14.8 ± 3.3
Ahr^{b1}Cyp1a2(−/−)		20.4 ± 2.5	19.3 ± 2.5	17.9 ± 2.7	14.2 ± 2.4	17.9 ± 2.8
Ahr^{d}Cyp1a2(−/−)		25.4 ± 5.2	24.3 ± 4.6	22.1 ± 4.4	17.3 ± 3.5	20.5 ± 3.8
Ahr^{b1}Cyp1a2(+/+)	Fetal liver	47.2 ± 5.5	34.9 ± 5.0	41.9 ± 5.3	26.3 ± 4.0	34.1 ± 4.5
Ahr^{d}Cyp1a2(+/+)		37.4 ± 7.7	26.6 ± 6.1	29.0 ± 6.8	19.4 ± 4.9	26.6 ± 7.2
Ahr^{b1}Cyp1a2(−/−)		36.9 ± 5.3	23.7 ± 3.9	28.3 ± 4.8	16.7 ± 3.3	24.2 ± 4.8
Ahr^{d}Cyp1a2(−/−)		37.6 ± 3.3	25.3 ± 2.1	30.0 ± 1.9	17.9 ± 1.4	25.3 ± 2.4

Note. These tissues were collected 8 days after the first gavage on GD10.5.

coplanar PCB 126 and PCB 169 were below the limits of detection in maternal and pup brain—for all four genotypes. All five noncoplanar congeners were remarkably similar when comparing the four genotypes in any of the eight tissues examined.

On PND13, 8 days after the second gavage (Tables 11 and 12), the coplanar PCB 77 was highest in *Cyp1a2(−/−)*-containing mouse lines for maternal inguinal fat pad and mammary tissues; PCB 77 was highest in *Ahr^{d}_Cyp1a2(−/−)* maternal brain and liver, as well as pup brain, liver, fat, and plasma compared with that of the other three genotypes. The coplanar PCB 126 and PCB 169 were below the limits of detection in maternal and pup brain and plasma—for all four genotypes. Again, all five noncoplanar congeners were remarkably similar when comparing the four genotypes in any of the eight tissues examined, except that *Ahr^{b1}Cyp1a2(−/−)* pups showed higher levels in all tissues at this time point.

On PND28, 23 days after the second gavage (Table 13), all three coplanar congeners were below the limits of detection in maternal brain, liver, mammary tissue (with exception of *Ahr^{d}_Cyp1a2(−/−)*), and in pup brain—for all four genotypes. Again, this finding indicates that the second dose on PND5 was being largely cleared from the tissues. Individual coplanar congeners were undetectable in various tissues of all four genotypes: PCB 126 in maternal inguinal fat pad and in pup liver and adipose tissue and PCB 77 in pup brain. Again, the coplanar PCB 77 was highest in *Ahr^{d}_Cyp1a2(−/−)* maternal inguinal fat pad and mammary tissue, as well as in pup liver, adipose tissue, and subcutaneous fat compared with that in the other three genotypes.

On PND28, all five noncoplanar congeners (Table 14) were remarkably similar when comparing the four genotypes in any of the eight tissues examined, with a few modest exceptions. Four of the five noncoplanar congeners were below the limits of detection in maternal brain; *Ahr^{d}_Cyp1a2(+/+)* was the exception, with four of the five noncoplanar PCBs detectable. PCB 118 is known to be readily metabolized, and it was below the level of detection in maternal liver for all genotypes except *Ahr^{b1}_Cyp1a2(−/−)*. For pup inguinal fat pad, all five noncoplanar congeners were highest in *Ahr^{b1}_Cyp1a2(−/−)*, and in pup subcutaneous fat, two of the five noncoplanars, PCB 105 and PCB 118, were highest in *Ahr^{d}_Cyp1a2(−/−)*.

The distribution of noncoplanar congeners from mother to pup closely matches their chlorination patterns: the more readily metabolized pentachlorobiphenyls were found at lower concentrations in the mothers and higher concentrations in their pups. In contrast, PCB 180, which is known to have an exceptionally long half-life (Oberg *et al.*, 2002), was still found at relatively high concentrations in maternal tissues. It is well known that if adjacent carbon atoms have no chlorine atoms,

TABLE 9
Coplanar PCB Congener Analysis on PND6

Genotype	Tissue	PCB 77	PCB 126	PCB 169
Ahr^{b1}Cyp1a2(+/+)	Maternal brain	0.7 ± 0.7	< 0.5	< 0.5
Ahr^{d}Cyp1a2(+/+)		9.8 ± 2.0	< 0.5	< 0.5
Ahr^{b1}Cyp1a2(−/−)		3.2 ± 0.8	< 0.5	< 0.5
Ahr^{d}Cyp1a2(−/−)		10.0 ± 1.1	< 0.5	< 0.5
Ahr^{b1}Cyp1a2(+/+)	Maternal liver	11.5 ± 1.8	3.1 ± 2.0	18.1 ± 1.9
Ahr^{d}Cyp1a2(+/+)		43.2 ± 8.8	0.7 ± 0.7	2.3 ± 0.6
Ahr^{b1}Cyp1a2(−/−)		10.0 ± 4.3	< 0.5	2.7 ± 1.6
Ahr^{d}Cyp1a2(−/−)		36.6 ± 6.0	< 0.5	1.3 ± 0.7
Ahr^{b1}Cyp1a2(+/+)	Maternal inguinal fat pad	122 ± 19	8.1 ± 0.2	43.6 ± 1.4
Ahr^{d}Cyp1a2(+/+)		271 ± 27	5.4 ± 1.8	34.5 ± 7.9
Ahr^{b1}Cyp1a2(−/−)		200 ± 7.9	1.7 ± 0.2	39.7 ± 5.4
Ahr^{d}Cyp1a2(−/−)		304 ± 11	4.4 ± 2.0	22.2 ± 1.7
Ahr^{b1}Cyp1a2(+/+)	Maternal mammary tissue	26.4 ± 14	0.8 ± 0.2	14.3 ± 4.1
Ahr^{d}Cyp1a2(+/+)		172 ± 36	4.1 ± 3.1	14.9 ± 5.5
Ahr^{b1}Cyp1a2(−/−)		64.8 ± 22	< 0.5	22.4 ± 6.8
Ahr^{d}Cyp1a2(−/−)		164 ± 36	1.2 ± 0.3	12.0 ± 0.7
Ahr^{b1}Cyp1a2(+/+)	Pup brain	1.2 ± 0.7	< 0.5	< 0.5
Ahr^{d}Cyp1a2(+/+)		11.6 ± 0.5	< 0.5	< 0.5
Ahr^{b1}Cyp1a2(−/−)		2.2 ± 0.1	< 0.5	< 0.5
Ahr^{d}Cyp1a2(−/−)		10.8 ± 1.0	< 0.5	< 0.5
Ahr^{b1}Cyp1a2(+/+)	Pup liver	30.5 ± 3.8	2.9 ± 2.0	24.7 ± 6.3
Ahr^{d}Cyp1a2(+/+)		59.5 ± 8.2	0.6 ± 0.3	4.2 ± 1.6
Ahr^{b1}Cyp1a2(−/−)		21.5 ± 1.6	0.8 ± 0.2	11.4 ± 4.5
Ahr^{d}Cyp1a2(−/−)		121 ± 28	0.7 ± 0.4	31.5 ± 7.9
Ahr^{b1}Cyp1a2(+/+)	Pup total adipose tissue	52.5 ± 10	1.4 ± 0.7	26.0 ± 3.3
Ahr^{d}Cyp1a2(+/+)		182 ± 30	2.8 ± 0.4	22.8 ± 9.1
Ahr^{b1}Cyp1a2(−/−)		109 ± 9.7	1.0 ± 0.3	18.8 ± 10
Ahr^{d}Cyp1a2(−/−)		339 ± 59	2.8 ± 1.4	20.5 ± 11
Ahr^{b1}Cyp1a2(+/+)	Pup stomach	48.4 ± 20	1.6 ± 0.9	15.6 ± 2.9
Ahr^{d}Cyp1a2(+/+)		169 ± 29	2.7 ± 1.3	10.5 ± 4.9
Ahr^{b1}Cyp1a2(−/−)		101 ± 13	0.7 ± 0.3	18.9 ± 2.7
Ahr^{d}Cyp1a2(−/−)		225 ± 26	1.8 ± 0.5	21.7 ± 4.3

Note. These tissues were collected 24 h after the second gavage on PND5.

then that PCB congener is more efficiently metabolized than congeners having no adjacent carbon atoms occupied with chlorine atoms. The pentachlorobiphenyls PCB 105 and 118 reached the highest levels in pups with lower concentrations of PCBs 138, 153, and 180; it is not clear why pentachlorinated congeners would persist in a tissue longer than hexa- and hepta-chlorinated congeners. *Ahr^{b1}_Cyp1a2(+/+)* dams were more effective at clearing both planar and noncoplanar congeners, continuing a trend first noted at GD11.5 for *Ahr^{b1}*-containing mice.

CYP1A1 and CYP1A2 mRNA Levels

Figure 5 depicts CYP1A1 and CYP1A2 mRNA levels—at the same five collection time points as carried out for congener analysis in Tables 5–14 as quantified by qRT-PCR. CYP1A1 mRNA was highly induced in *Ahr^{b1}_Cyp1a2(+/+)* maternal liver on GD11.5, GD18.5, PND6, and PND13 but not PND28. CYP1A1 mRNA was highly induced in *Ahr^{b1}_Cyp1a2(−/−)* maternal liver at all five time points, including PND28. CYP1A1 mRNA was not significantly induced in *Ahr^{d}_Cyp1a2(+/+)* or *Ahr^{d}_Cyp1a2(−/−)* maternal liver at any of the five time points.

CYP1A1 mRNA showed an increased trend, but not statistically significant ($p > 0.05$), in *Ahr^{b1}_Cyp1a2(+/+)* whole embryo on GD11.5 (Fig. 5A). CYP1A1 mRNA was highly induced in *Ahr^{b1}_Cyp1a2(+/+)* and *Ahr^{b1}_Cyp1a2(−/−)* fetal liver on GD18.5 (Figs. 5A and 5B), as well as in pup liver on PND6, PND13, and PND28 (Figs. 5C, 5D, and 5E). CYP1A1 mRNA showed an increased trend, but was not statistically significant ($p > 0.05$), in *Ahr^{b1}_Cyp1a2(+/+)* pup brain at PND28, whereas CYP1A1 mRNA was statistically significantly induced in *Ahr^{b1}_Cyp1a2(−/−)* pup brain at PND28 (Fig. 5E).

CYP1A2 mRNA was significantly induced in maternal liver of *Ahr^{b1}_Cyp1a2(+/+)* at GD11.5, GD18.5, PND6, and PND13 (Figs. 5A, 5B, 5C, and 5D). CYP1A2 mRNA was

TABLE 10
Noncoplanar PCB Congener Analysis on PND6

Genotype	Tissue	PCB 105	PCB 118	PCB 138	PCB 153	PCB 180
Ahr^{b1}Cyp1a2(+/+)	Maternal brain	17.7 ± 1.4	17.2 ± 1.6	18.6 ± 1.4	16.9 ± 1.3	32.1 ± 1.6
Ahr^{d}Cyp1a2(+/+)		26.2 ± 2.9	24.5 ± 3.2	25.6 ± 3.6	21.9 ± 3.6	40.0 ± 4.2
Ahr^{b1}Cyp1a2(−/−)		24.2 ± 2.2	22.7 ± 2.0	22.5 ± 2.9	20.4 ± 3.2	36.9 ± 3.2
Ahr^{d}Cyp1a2(−/−)		17.2 ± 2.2	15.6 ± 2.2	17.8 ± 3.3	17.2 ± 2.9	30.5 ± 5.2
Ahr^{b1}Cyp1a2(+/+)	Maternal liver	79.2 ± 8.8	60.8 ± 7.4	70.6 ± 5.4	41.9 ± 4.4	81.8 ± 4.0
Ahr^{d}Cyp1a2(+/+)		95.6 ± 14	70.6 ± 13	76.6 ± 13	51.0 ± 10	86.6 ± 15
Ahr^{b1}Cyp1a2(−/−)		82.7 ± 14	59.5 ± 13	72.2 ± 14	45.4 ± 14	85.3 ± 20
Ahr^{d}Cyp1a2(−/−)		71.6 ± 13	50.3 ± 10	62.1 ± 10	39.0 ± 8.3	76.5 ± 15
Ahr^{b1}Cyp1a2(+/+)	Maternal inguinal fat pad	538 ± 29	507 ± 18	536 ± 16	450 ± 13	524 ± 22
Ahr^{d}Cyp1a2(+/+)		586 ± 54	545 ± 59	488 ± 41	414 ± 44	445 ± 33
Ahr^{b1}Cyp1a2(−/−)		642 ± 16	585 ± 13	569 ± 16	460 ± 11	521 ± 25
Ahr^{d}Cyp1a2(−/−)		464 ± 52	463 ± 12	441 ± 42	376 ± 29	428 ± 29
Ahr^{b1}Cyp1a2(+/+)	Maternal mammary tissue	267 ± 66	246 ± 61	240 ± 52	189 ± 41	268 ± 33
Ahr^{d}Cyp1a2(+/+)		377 ± 48	346 ± 44	338 ± 42	249 ± 34	320 ± 28
Ahr^{b1}Cyp1a2(−/−)		285 ± 49	259 ± 46	249 ± 45	188 ± 36	252 ± 28
Ahr^{d}Cyp1a2(−/−)		256 ± 27	215 ± 16	223 ± 15	182 ± 28	250 ± 31
Ahr^{b1}Cyp1a2(+/+)	Pup brain	29.6 ± 4.5	27.6 ± 3.4	27.1 ± 4.8	22.6 ± 3.9	31.6 ± 7.4
Ahr^{d}Cyp1a2(+/+)		32.4 ± 4.8	32.2 ± 5.2	28.9 ± 5.2	24.0 ± 4.4	30.0 ± 4.8
Ahr^{b1}Cyp1a2(−/−)		25.9 ± 3.5	24.4 ± 3.1	19.1 ± 2.7	17.5 ± 2.1	22.0 ± 3.5
Ahr^{d}Cyp1a2(−/−)		19.5 ± 2.1	18.0 ± 0.8	17.3 ± 1.6	14.9 ± 1.3	21.1 ± 3.6
Ahr^{b1}Cyp1a2(+/+)	Pup liver	235 ± 52	209 ± 47	210 ± 42	164 ± 34	254.8 ± 45
Ahr^{d}Cyp1a2(+/+)		156 ± 28	123 ± 26	117 ± 21	101 ± 23	145 ± 26
Ahr^{b1}Cyp1a2(−/−)		271 ± 25	235 ± 23	220 ± 19	178 ± 16	246.0 ± 18
Ahr^{d}Cyp1a2(−/−)		269 ± 40	233 ± 37	243 ± 38	198 ± 32	297 ± 40
Ahr^{b1}Cyp1a2(+/+)	Pup total adipose tissue	508 ± 25	454 ± 23	417 ± 19	317 ± 11	343 ± 12
Ahr^{d}Cyp1a2(+/+)		434 ± 81	378 ± 74	351 ± 73	269 ± 52	279 ± 67
Ahr^{b1}Cyp1a2(−/−)		626 ± 42	547 ± 39	487 ± 38	371 ± 30	384 ± 38
Ahr^{d}Cyp1a2(−/−)		543 ± 43	475 ± 40	406 ± 35	326 ± 29	318 ± 36
Ahr^{b1}Cyp1a2(+/+)	Pup stomach	329 ± 11	291 ± 2.0	272 ± 8.0	206 ± 10	253 ± 15
Ahr^{d}Cyp1a2(+/+)		353 ± 51	307 ± 49	270 ± 46	205 ± 38	242 ± 36
Ahr^{b1}Cyp1a2(−/−)		348 ± 23	305 ± 22	271 ± 20	211 ± 15	253 ± 24
Ahr^{d}Cyp1a2(−/−)		347 ± 47	300 ± 41	287 ± 41	224 ± 34	273 ± 42

Note. These tissues were collected 24 h after the second gavage on PND5.

not detectable in whole embryo at GD11.5 but was significantly increased in *Ahr^{b1}_Cyp1a2(+/+)* fetal liver at GD18.5 (Fig. 5B). CYP1A2 mRNA was also significantly induced in *Ahr^{b1}_Cyp1a2(+/+)* pup liver at PND6, PND13, and PND28. CYP1A2 mRNA was not detectable in *Ahr^{d}_Cyp1a2(+/+)* embryonic or fetal liver (GD11.5 and GD18.5) or neonatal liver on PND6, but there was a trend of increase that was not significant ($p > 0.05$) at PND13, and the induction was statistically significant ($p < 0.05$) at PND28.

Evidence of Immunosuppression and AHR Activation

Oral BaP is well known to cause immunosuppression, even at quite low daily doses (Uno *et al.*, 2004). We therefore wondered if the PCB mixture, perhaps especially the coplanar PCBs operating via AHR-mediated downstream effects, might cause toxic effects of the immune system in the neonate and weanling—following the two gavage treatments of the PCB mixture at GD10.5 and PND5.

Whereas no significant splenic atrophy was seen at PND6 (Fig. 6A), a statistically significant decrease was observed on PND13 in *Ahr^{b1}_Cyp1a2(−/−)* pups. Statistically significant splenic atrophy was found at PND28 in *Ahr^{b1}_Cyp1a2(+/+)* pups, whereas a trend of decreased spleen weight that was not statistically significant ($p > 0.05$) was noted in all the three other genotypes (Fig. 6A). Immunosuppression in the offspring thus appears to be associated with the *Ahr^{b1}* phenotype combined with the presence of maternal hepatic CYP1A2.

Thymic atrophy was statistically significant ($p < 0.001$) in both *Ahr^{b1}*-containing mouse lines at PND6, PND13, and PND28 (Fig. 6B). Statistically significant ($p < 0.05$) decreases in thymus weights were also seen in both *Ahr^{d}*-containing mouse lines at PND13. The fact that thymic atrophy was not so striking at PND28 suggests that the concentrations of coplanar PCBs might have been diminished by this time—which is consistent with the data in Tables 13 and 14. Thymic

TABLE 11
Coplanar PCB Congener Analysis on PND13*

Genotype	Tissue	PCB 77	PCB 126	PCB 169
Ahr^{b1}Cyp1a2(+/+)	Maternal brain	< 0.5	< 0.5	< 0.5
Ahr^{d}Cyp1a2(+/+)		0.5 ± 0.5	< 0.5	< 0.5
Ahr^{b1}Cyp1a2(−/−)		< 0.5	< 0.5	< 0.5
Ahr^{d}Cyp1a2(−/−)		1.7 ± 0.6	< 0.5	< 0.5
Ahr^{b1}Cyp1a2(+/+)	Maternal liver	< 0.5	4.5 ± 1.4	2.4 ± 0.7
Ahr^{d}Cyp1a2(+/+)		< 0.5	< 0.5	< 0.5
Ahr^{b1}Cyp1a2(−/−)		0.9 ± 0.5	< 0.5	< 0.5
Ahr^{d}Cyp1a2(−/−)		1.5 ± 0.1	< 0.5	< 0.5
Ahr^{b1}Cyp1a2(+/+)	Maternal inguinal fat pad	3.3 ± 2.1	1.0 ± 0.6	35.6 ± 11
Ahr^{d}Cyp1a2(+/+)		10.4 ± 0.8	1.2 ± 0.8	34.9 ± 1.8
Ahr^{b1}Cyp1a2(−/−)		33.9 ± 6.1	5.3 ± 2.9	69.4 ± 11
Ahr^{d}Cyp1a2(−/−)		35.9 ± 12	0.9 ± 0.6	15.0 ± 8.8
Ahr^{b1}Cyp1a2(+/+)	Maternal mammary tissue	< 0.5	< 0.5	1.8 ± 1.1
Ahr^{d}Cyp1a2(+/+)		1.2 ± 0.2	< 0.5	1.9 ± 0.3
Ahr^{b1}Cyp1a2(−/−)		3.1 ± 0.6	< 0.5	10.8 ± 2.4
Ahr^{d}Cyp1a2(−/−)		3.2 ± 0.6	< 0.5	< 0.5
Ahr^{b1}Cyp1a2(+/+)	Pup brain	< 0.5	< 0.5	< 0.5
Ahr^{d}Cyp1a2(+/+)		3.1 ± 1.0	< 0.5	< 0.5
Ahr^{b1}Cyp1a2(−/−)		< 0.5	< 0.5	< 0.5
Ahr^{d}Cyp1a2(−/−)		13.6 ± 6.9	< 0.5	< 0.5
Ahr^{b1}Cyp1a2(+/+)	Pup liver	1.0 ± 0.7	22.6 ± 4.1	31.9 ± 3.1
Ahr^{d}Cyp1a2(+/+)		11.6 ± 2.7	1.2 ± 0.6	2.3 ± 0.3
Ahr^{b1}Cyp1a2(−/−)		0.9 ± 0.5	1.2 ± 0.4	11.6 ± 1.7
Ahr^{d}Cyp1a2(−/−)		46.5 ± 16	< 0.5	1.4 ± 1.2
Ahr^{b1}Cyp1a2(+/+)	Pup total adipose tissue	2.4 ± 0.7	2.1 ± 0.5	50.0 ± 4.8
Ahr^{d}Cyp1a2(+/+)		106 ± 16	6.4 ± 0.5	40.7 ± 4.1
Ahr^{b1}Cyp1a2(−/−)		19.1 ± 1.0	14.4 ± 1.0	96.0 ± 6.3
Ahr^{d}Cyp1a2(−/−)		408 ± 32	3.6 ± 1.5	24.7 ± 12
Ahr^{b1}Cyp1a2(+/+)	Pup plasma	< 0.5	< 0.5	< 0.5
Ahr^{d}Cyp1a2(+/+)		2.0 ± 0.2	< 0.5	< 0.5
Ahr^{b1}Cyp1a2(−/−)		< 0.5	< 0.5	< 0.5
Ahr^{d}Cyp1a2(−/−)		8.2 ± 0.8	< 0.5	< 0.5

Note. These tissues were collected 8 days after the second gavage to the mother on PND5.

atrophy can be caused by chronic AHR activation, which would occur by repeated administration of the PCB mixture. This would explain why the *Ahr^{b1}* phenotype is more important than the presence or absence of maternal hepatic CYP1A2.

The liver weight to total body weight ratio was dramatically increased in all four PCB-treated genotypes at PND6 ($p < 0.001$) compared with that in controls receiving no PCBs (Fig. 6C); this ratio is also caused by chronic AHR activation. The liver weight to total body weight ratio was significantly ($p < 0.001$) increased in the two *Ahr^{b1}*-containing mouse lines at PND13 ($p < 0.001$) but only in *Ahr^{b1}_Cyp1a2(−/−)* weanlings at PND28 ($p < 0.001$).

Mothers at PND28 were sacrificed and organ weights obtained. Spleen weights were trending downward in *Cyp1a2(−/−)* mothers, but the data were not significantly different ($p > 0.05$) from that in *Cyp1a2(+/+)* mothers. Thymus weights were trending lower, and liver weight to total body weight ratios were trending upward in *Ahr^{b1}*-containing mothers, but again these results were not significantly different ($p > 0.05$) from that in *Ahr^{d}*-containing mothers (data not illustrated).

DISCUSSION

In the present study, we have shown that genetic differences in AHR affinity, as well as the presence or absence of the CYP1A2 enzyme, influence the maternal-fetal unit—with regard to PCB congener pharmacokinetics and degrees of toxic response to the developing neonate and weanling mouse. Our initial goal was to decide upon a PCB mixture that not only reflected that found in human breast milk and other tissues and a dose that would activate AHR but also a PCB dosage exposure that was neither substantially lethal nor causing overt birth defects such as cleft palate and hydronephrosis. Our long-range goal was to study behavioral phenotypes in these offspring when they reached adulthood at PND60, and this is the subject of the next paper (Curran, Genter, Patel, Vorhees, Williams, and Nebert, in preparation).

TABLE 12
Noncoplanar PCB Congener Analysis on PND13

Genotype	Tissue	PCB 105	PCB 118	PCB 138	PCB 153	PCB 180
Ahr^{b1}Cyp1a2(+/+)	Maternal brain	8.96 ± 4.2	8.07 ± 3.9	10.0 ± 4.1	7.69 ± 2.9	11.6 ± 3.4
Ahr^{d}Cyp1a2(+/+)		5.22 ± 0.70	4.36 ± 0.93	5.00 ± 1.2	4.31 ± 1.1	6.55 ± 1.9
Ahr^{b1}Cyp1a2(−/−)		9.45 ± 3.9	8.48 ± 3.9	10.1 ± 4.3	8.33 ± 3.2	13.9 ± 4.5
Ahr^{d}Cyp1a2(−/−)		3.65 ± 1.3	3.26 ± 1.4	3.97 ± 1.3	3.63 ± 1.1	6.59 ± 2.2
Ahr^{b1}Cyp1a2(+/+)	Maternal liver	16.0 ± 4.8	10.8 ± 3.4	37.6 ± 7.9	13.3 ± 3.8	52.0 ± 7.8
Ahr^{d}Cyp1a2(+/+)		17.8 ± 3.6	11.4 ± 3.0	36.4 ± 7.5	13.4 ± 3.6	47.0 ± 10
Ahr^{b1}Cyp1a2(−/−)		41.3 ± 19	25.9 ± 12	58.3 ± 12	24.3 ± 8.6	70.7 ± 2.5
Ahr^{d}Cyp1a2(−/−)		8.65 ± 0.75	4.50 ± 0.54	26.4 ± 1.4	6.31 ± 0.69	39.1 ± 4.4
Ahr^{b1}Cyp1a2(+/+)	Maternal inguinal fat pad	188 ± 79	213 ± 79	333 ± 96	303 ± 82	448 ± 88
Ahr^{d}Cyp1a2(+/+)		249 ± 38	270 ± 46	400 ± 66	356 ± 58	469 ± 21
Ahr^{b1}Cyp1a2(−/−)		393 ± 170	353 ± 120	507 ± 95	440 ± 49	625 ± 26
Ahr^{d}Cyp1a2(−/−)		235 ± 54	278 ± 53	424 ± 59	382 ± 45	525 ± 47
Ahr^{b1}Cyp1a2(+/+)	Maternal mammary tissue	21.1 ± 9.3	24.3 ± 10	38.7 ± 15	32.0 ± 12	66.7 ± 24
Ahr^{d}Cyp1a2(+/+)		27.1 ± 3.6	30.5 ± 5.0	44.1 ± 7.5	36.1 ± 5.9	74.7 ± 8.2
Ahr^{b1}Cyp1a2(−/−)		113 ± 36	113 ± 33	155 ± 36	132 ± 24	246 ± 27
Ahr^{d}Cyp1a2(−/−)		11.3 ± 2.3	14.2 ± 2.9	24.8 ± 4.6	21.3 ± 3.8	53.6 ± 11.1
Ahr^{b1}Cyp1a2(+/+)	Pup brain	23.2 ± 3.8	21.1 ± 2.9	23.5 ± 4.0	18.2 ± 3.3	23.9 ± 4.3
Ahr^{d}Cyp1a2(+/+)		27.8 ± 6.1	23.9 ± 5.8	21.0 ± 5.3	16.3 ± 3.9	19.0 ± 4.8
Ahr^{b1}Cyp1a2(−/−)		47.9 ± 4.5	41.4 ± 5.6	37.8 ± 3.6	29.0 ± 2.9	37.0 ± 3.7
Ahr^{d}Cyp1a2(−/−)		23.7 ± 8.5	20.9 ± 6.9	18.1 ± 6.2	14.6 ± 5.0	16.6 ± 5.3
Ahr^{b1}Cyp1a2(+/+)	Pup liver	98.6 ± 8.6	79.6 ± 6.3	77.6 ± 6.6	48.2 ± 4.8	68.2 ± 7.1
Ahr^{d}Cyp1a2(+/+)		64.7 ± 1.3	51.3 ± 7.4	52.8 ± 11	36.9 ± 11	49.1 ± 13
Ahr^{b1}Cyp1a2(−/−)		231 ± 33	181 ± 28	175 ± 24	123 ± 22	161 ± 21
Ahr^{d}Cyp1a2(−/−)		77.8 ± 25	58.1 ± 19	58.1 ± 19	39.0 ± 14	50.7 ± 18
Ahr^{b1}Cyp1a2(+/+)	Pup total adipose tissue	624 ± 70	558 ± 57	562 ± 56	442 ± 42	482 ± 42
Ahr^{d}Cyp1a2(+/+)		594 ± 120	518 ± 88	501 ± 72	412 ± 37	429 ± 48
Ahr^{b1}Cyp1a2(−/−)		740 ± 26	691 ± 38	651 ± 26	497 ± 12	551 ± 12
Ahr^{d}Cyp1a2(−/−)		636 ± 34	566 ± 27	535 ± 26	428 ± 25	459 ± 30
Ahr^{b1}Cyp1a2(+/+)	Pup plasma	17.9 ± 3.8	16.7 ± 3.3	17.8 ± 3.3	15.3 ± 3.4	16.9 ± 2.9
Ahr^{d}Cyp1a2(+/+)		15.6 ± 1.0	13.7 ± 0.84	11.5 ± 0.8	9.7 ± 0.7	9.6 ± 1.0
Ahr^{b1}Cyp1a2(−/−)		35.7 ± 2.1	34.1 ± 1.3	28.8 ± 1.2	24.3 ± 0.8	28.2 ± 0.4
Ahr^{d}Cyp1a2(−/−)		11.8 ± 0.9	11.2 ± 0.9	9.6 ± 0.8	8.8 ± 0.4	7.9 ± 0.4

Note. These tissues were collected 8 days after the second gavage to the mother on PND5.

We were aware of studies using Aroclor mixtures that have repeatedly described neurological deficits across rodent species (Chishti *et al*., 1996; Kang *et al*., 2002). However, when attempts were made to identify individual congeners responsible for these effects, it became clear that single congeners did not produce the wide-ranging effects reported when studying Aroclor mixtures in laboratory animal studies, as well as effects observed in human cohorts (Ulbrich and Stahlmann, 2004); this suggests that a mixture of congeners, rather than individual congeners, might be responsible for PCB-induced developmental neurotoxicity. In fact, other researchers reported that a mixture of coplanar plus noncoplanar PCB congeners was required to elicit changes in thyroid hormone signaling in the developing brain (Gauger *et al*., 2004). For all these reasons, we decided to use the eight PCB complex mixture listed in Table 1, with chemical structures depicted in Figure 1.

Preliminary studies also confirmed that we needed to provide a booster dose of the PCB mixture—in order to maintain high CYP1A1 mRNA inducibility (as a measure of chronic AHR activation) and sufficient PCB congener concentrations in the various tissues of the pup. Hence, we chose the regimen of one dose of PCBs given on GD10.5 and a second dose on PND5; collection time points for analysis included GD11.5, GD18.5, PND6, PND13, and PND28. The time line for our entire experimental paradigm is summarized in Figure 2.

We then wished to test differences in response to the PCB mixture in mice having the high-affinity versus poor-affinity AHR combined with the presence versus absence of CYP1A2. Previous work from this laboratory had convincingly shown that presence of maternal hepatic CYP1A2 was able to sequester TCDD such that the fetus was protected approximately sixfold more than fetuses from mothers lacking hepatic CYP1A2; this led, in *Cyp1a2(−/−)* mothers, to an approximately six times larger dose of TCDD required to cause cleft

TABLE 13
Coplanar PCB Congener Analysis on PND28

Genotype	Tissue	PCB 77	PCB 126	PCB 169
Ahr^{b1}Cyp1a2(+/+)	Maternal brain	< 0.5	< 0.5	< 0.5
Ahr^{d}Cyp1a2(+/+)		< 0.5	< 0.5	< 0.5
Ahr^{b1}Cyp1a2(−/−)		< 0.5	< 0.5	< 0.5
Ahr^{d}Cyp1a2(−/−)		< 0.5	< 0.5	< 0.5
Ahr^{b1}Cyp1a2(+/+)	Maternal liver	< 0.5	< 0.5	< 0.5
Ahr^{d}Cyp1a2(+/+)		< 0.5	< 0.5	< 0.5
Ahr^{b1}Cyp1a2(−/−)		< 0.5	< 0.5	< 0.5
Ahr^{d}Cyp1a2(−/−)		< 0.5	< 0.5	< 0.5
Ahr^{b1}Cyp1a2(+/+)	Maternal inguinal fat pad	< 0.5	< 0.5	< 0.5
Ahr^{d}Cyp1a2(+/+)		< 0.5	< 0.5	< 0.5
Ahr^{b1}Cyp1a2(−/−)		< 0.5	< 0.5	8.5 ± 1.3
Ahr^{d}Cyp1a2(−/−)		6.5 ± 4.0	< 0.5	8.4 ± 4.4
Ahr^{b1}Cyp1a2(+/+)	Maternal mammary tissue	< 0.5	< 0.5	< 0.5
Ahr^{d}Cyp1a2(+/+)		< 0.5	< 0.5	< 0.5
Ahr^{b1}Cyp1a2(−/−)		< 0.5	< 0.5	< 0.5
Ahr^{d}Cyp1a2(−/−)		5.2 ± 3.2	< 0.5	< 0.5
Ahr^{b1}Cyp1a2(+/+)	Pup brain	< 0.5	< 0.5	< 0.5
Ahr^{d}Cyp1a2(+/+)		< 0.5	< 0.5	< 0.5
Ahr^{b1}Cyp1a2(−/−)		< 0.5	< 0.5	< 0.5
Ahr^{d}Cyp1a2(−/−)		< 0.5	< 0.5	< 0.5
Ahr^{b1}Cyp1a2(+/+)	Pup liver	< 0.5	< 0.5	3.6 ± 1.9
Ahr^{d}Cyp1a2(+/+)		< 0.5	< 0.5	< 0.5
Ahr^{b1}Cyp1a2(−/−)		< 0.5	< 0.5	< 0.5
Ahr^{d}Cyp1a2(−/−)		20.0 ± 5.3	< 0.5	< 0.5
Ahr^{b1}Cyp1a2(+/+)	Pup subcutaneous adipose tissue	< 0.5	< 0.5	11.5 ± 1.7
Ahr^{d}Cyp1a2(+/+)		< 0.5	< 0.5	18.5 ± 2.9
Ahr^{b1}Cyp1a2(−/−)		< 0.5	< 0.5	18.2 ± 0.2
Ahr^{d}Cyp1a2(−/−)		182 ± 60	< 0.5	19.2 ± 1.9
Ahr^{b1}Cyp1a2(+/+)	Pup inguinal fat pad	< 0.5	< 0.5	12.7 ± 0.4
Ahr^{d}Cyp1a2(+/+)		< 0.5	2.2 ± 1.3	24.4 ± 6.2
Ahr^{b1}Cyp1a2(−/−)		< 0.5	4.2 ± 0.8	41.2 ± 13
Ahr^{d}Cyp1a2(−/−)		243 ± 37	< 0.5	22.0 ± 2.3

Note. These tissues were collected 23 days after the second gavage of the mother on PND5.

palate and hydronephrosis (Dragin *et al*., 2006). It is also well known that *Ahr^{d}*-containing mice require a 15- to 20-fold higher dose of TCDD in order to achieve the same level of CYP1 inducibility as that seen in *Ahr^{b1}*-containing mice (Poland *et al*., 1974). Combining these facts, we hypothesized that the *Ahr^{b1}_Cyp1a2(−/−)* mother-fetal unit would be most vulnerable, the *Ahr^{d}_Cyp1a2(−/−)* unit would be almost as vulnerable, the *Ahr^{b1}_Cyp1a2(+/+)* unit would be most resistant, and the *Ahr^{d}_Cyp1a2(+/+)* would be almost as resistant—with regard to toxicity induced by the PCB mixture (Table 3).

True to our predictions, small but statistically significant PCB-induced decreases in newborn birth weights were found in both *Cyp1a2(−/−)*-containing lines (Table 4) and a small but statistically significant PCB-induced decreased growth rate was seen in *Ahr^{b1}_Cyp1a2(−/−)* pups between PND1 and PND28 (Fig. 3). In general, noncoplanar congener concentrations in mother and offspring tissues between GD11.5 and PND28 were not associated with the *Ahr* or *Cyp1a2* genotype (Tables 5–14)—except for *Ahr^{b1}_Cyp1a2(−/−)* PND13 pups exhibiting higher levels in all tissues (Table 12), all five noncoplanar congeners highest in *Ahr^{b1}_Cyp1a2(−/−)* PND28 pup inguinal fat pad (Table 14), and PCB 105 and PCB 118 highest in *Ahr^{d}_Cyp1a2(−/−)* PND28 pup subcutaneous fat (Table 14).

However, the coplanar PCB congeners did show an intriguing pattern: at various collection time points, the *Ahr^{d}_Cyp1a2(−/−)* maternal brain, liver, adipose, and mammary tissues (as well as placenta, fetal, and neonatal tissues) retained the most coplanar PCB 77—until PND28 when most coplanar congeners had been metabolically cleared from the tissues (Table 13). Thus, protection of the fetus by maternal hepatic CYP1A2 in *Ahr^{b1}_Cyp1a2(+/+)* mice, after the PND5 dose given to the mother, continues through lactation and is associated with the high-affinity

TABLE 14
Noncoplanar PCB Congener Analysis on PND28

Genotype	Tissue	PCB 105	PCB 118	PCB 138	PCB 153	PCB 180
Ahr^{b1}Cyp1a2(+/+)	Maternal brain	< 0.5	< 0.5	< 0.5	< 0.5	< 0.5
Ahr^{d}Cyp1a2(+/+)		< 0.5	3.5 ± 2.3	7.6 ± 5.0	6.7 ± 4.7	18.4 ± 13
Ahr^{b1}Cyp1a2(−/−)		< 0.5	< 0.5	< 0.5	< 0.5	2.9 ± 0.8
Ahr^{d}Cyp1a2(−/−)		< 0.5	< 0.5	< 0.5	< 0.5	< 0.5
Ahr^{b1}Cyp1a2(+/+)	Maternal liver	0.6 ± 0.4	< 0.5	5.8 ± 3.2	1.8 ± 1.1	17.9 ± 4.2
Ahr^{d}Cyp1a2(+/+)		6.3 ± 3.2	< 0.5	18.0 ± 7.7	9.8 ± 5.7	32.7 ± 9.7
Ahr^{b1}Cyp1a2(−/−)		4.7 ± 0.8	2.5 ± 1.2	14.8 ± 3.3	5.2 ± 1.5	27.4 ± 2.7
Ahr^{d}Cyp1a2(−/−)		4.0 ± 2.3	< 0.5	13.5 ± 4.9	5.1 ± 2.6	23.0 ± 5.4
Ahr^{b1}Cyp1a2(+/+)	Maternal inguinal fat pad	3.9 ± 2.0	7.2 ± 3.0	27.8 ± 9.1	36.5 ± 10	119 ± 17
Ahr^{d}Cyp1a2(+/+)		44.2 ± 31	57.2 ± 39	126 ± 73	134 ± 64	272 ± 81
Ahr^{b1}Cyp1a2(−/−)		31.7 ± 11	41.9 ± 16	95.7 ± 26	112 ± 23	233 ± 15
Ahr^{d}Cyp1a2(−/−)		34.7 ± 22	48.1 ± 29	112 ± 56	118 ± 49	230 ± 59
Ahr^{b1}Cyp1a2(+/+)	Maternal mammary tissue	14.1 ± 9.7	19.2 ± 13	43.5 ± 26	48.2 ± 29	104 ± 60
Ahr^{d}Cyp1a2(+/+)		10.0 ± 0.5	12.7 ± 0.7	22.7 ± 3.2	25.6 ± 2.9	59.3 ± 3.3
Ahr^{b1}Cyp1a2(−/−)		19.0 ± 7.8	24.3 ± 11	47.4 ± 21	51.3 ± 22	103 ± 34
Ahr^{d}Cyp1a2(−/−)		18.4 ± 11	22.7 ± 14	46.3 ± 27	44.0 ± 24	75.5 ± 36
Ahr^{b1}Cyp1a2(+/+)	Pup brain	5.7 ± 1.4	5.9 ± 1.3	8.0 ± 2.1	6.0 ± 2.4	6.9 ± 2.0
Ahr^{d}Cyp1a2(+/+)		12.1 ± 3.7	12.1 ± 4.1	15.1 ± 7.5	10.9 ± 5.4	13.6 ± 7.6
Ahr^{b1}Cyp1a2(−/−)		15.2 ± 1.4	13.4 ± 1.3	13.0 ± 1.2	8.8 ± 0.6	12.5 ± 2.2
Ahr^{d}Cyp1a2(−/−)		14.9 ± 2.9	12.5 ± 2.8	10.9 ± 2.5	10.1 ± 2.0	9.4 ± 2.7
Ahr^{b1}Cyp1a2(+/+)	Pup liver	24.3 ± 1.3	18.2 ± 1.0	29.9 ± 1.9	14.5 ± 0.9	23.0 ± 1.7
Ahr^{d}Cyp1a2(+/+)		41.2 ± 3.8	29.5 ± 5.6	38.0 ± 8.6	21.2 ± 5.7	27.9 ± 7.6
Ahr^{b1}Cyp1a2(−/−)		60.8 ± 5.9	39.4 ± 3.1	43.1 ± 5.6	26.4 ± 2.4	35.7 ± 2.8
Ahr^{d}Cyp1a2(−/−)		40.2 ± 7.4	23.3 ± 5.1	28.8 ± 4.3	15.8 ± 2.3	20.3 ± 2.8
Ahr^{b1}Cyp1a2(+/+)	Pup subcutaneous adipose tissue	198 ± 10	192 ± 6.9	236 ± 14	180 ± 6.1	183 ± 13
Ahr^{d}Cyp1a2(+/+)		342 ± 44	311 ± 49	336 ± 48	259 ± 37	291 ± 60
Ahr^{b1}Cyp1a2(−/−)		369 ± 23	312 ± 21	293 ± 15	233 ± 13	218 ± 3.6
Ahr^{d}Cyp1a2(−/−)		407 ± 26	343 ± 22	321 ± 17	259 ± 17	236 ± 17
Ahr^{b1}Cyp1a2(+/+)	Pup inguinal fat pad	200 ± 16	199 ± 11	247 ± 10	200 ± 8.9	224 ± 8.2
Ahr^{d}Cyp1a2(+/+)		386 ± 71	341 ± 62	355 ± 63	289 ± 50	302 ± 55
Ahr^{b1}Cyp1a2(−/−)		584 ± 94	502 ± 74	487 ± 75	408 ± 58	428 ± 100
Ahr^{d}Cyp1a2(−/−)		430 ± 59	376 ± 49	370 ± 51	306 ± 31	298 ± 32

Note. These tissues were collected 23 days after the second gavage of the mother on PND5.

AHR. Our data are consistent with previous findings that the greatest exposure to pups is during lactation—not during gestation (Seegal *et al*., 1997).

Figure 5 depicts CYP1A1 and CYP1A2 mRNA levels—at the same five collection time points as carried out for congener analysis in Tables 5–14—as quantified by qRT-PCR. CYP1A1 mRNA was highly induced in *Ahr^{b1}_Cyp1a2(+/+)* maternal liver on GD11.5, GD18.5, PND6, and PND13 but not PND28; disappearance on PND28 is consistent with the coplanar PCBs being mostly sequestered by maternal liver CYP1A2. In support of this hypothesis, CYP1A1 mRNA was highly induced in *Ahr^{b1}_Cyp1a2(−/−)* maternal liver at all five time points, including PND28, because of no maternal liver CYP1A2 to tie up the coplanar PCB inducers. CYP1A1 mRNA was not significantly induced in *Ahr^{d}_Cyp1a2(+/+)* or *Ahr^{d}_Cyp1a2(+/+)* maternal liver at any of the five time points; these observations are consistent with what is generally seen in *Ahr^{d}*-containing mouse lines (Nebert *et al*., 1972).

Western blots of CYP1A1 and CYP1A2 protein could have been carried out in all the tissues in which qRT-PCR measurements of CYP1A1 and CYP1A2 mRNA levels were obtained because it is always possible that protein levels might not reflect mRNA levels. However, in several dozen studies from this laboratory (Uno *et al*., 2008 and references therein), there has never been an instance in which CYP1 protein levels did not accurately reflect CYP1 mRNA levels.

An important next step in future studies would be to determine the concentration, identity, and transfer of PCB metabolites produced during gestation and lactation. Does the reduction in lower molecular weight congeners represent true clearance or simply the biotransformation into potentially toxic metabolites (Kimura-Kuroda *et al*., 2005)? This is an important question because hydroxylated and

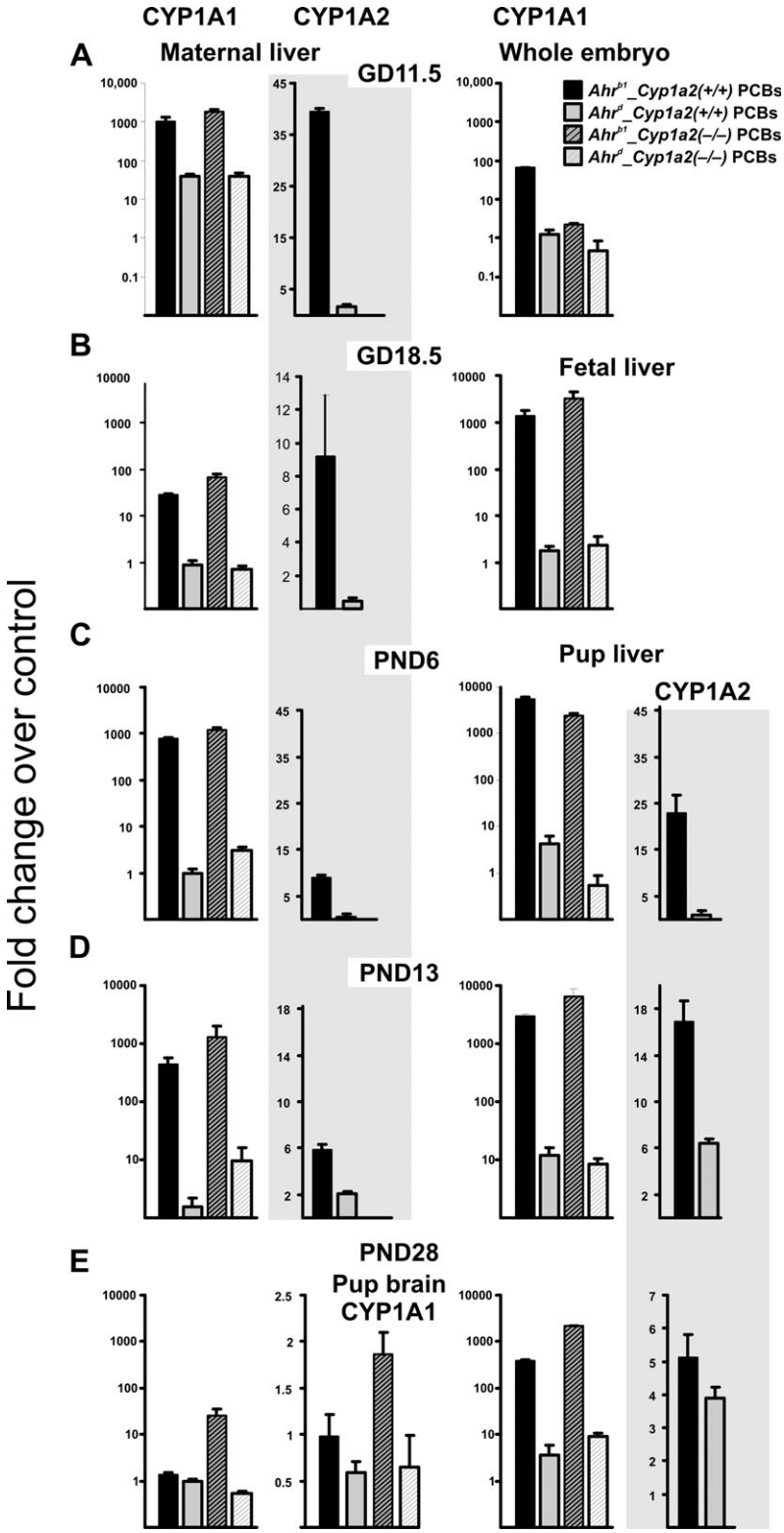

FIG. 5 CYP1A1 and CYP1A2 mRNA levels, quantified by qRT-PCR. (Top row) GD11.5. CYP1A1 induction was significantly higher in Ahr^{b1}-containing maternal liver compared with Ahr^{d}-containing mothers. CYP1A2 mRNA levels were 40-fold higher in Ahr^{b1}*_Cyp1a2(+/+)* maternal liver compared with Ahr^{d}*_Cyp1a2(+/+)* mothers. In this and in subsequent panels, all values represent mean values of fold induction over corn oil–treated B6 controls ± SEM. $N =$ 3–5 per group. Interindividual and group statistics are available upon request. (Second row) GD18.5. CYP1A1 induction was significantly higher in Ahr^{b1}-containing maternal and pup liver compared with Ahr^{d}-containing mothers and pups. CYP1A2 mRNA levels were ~10-fold higher in Ahr^{b1}*_Cyp1a2(+/+)* maternal liver

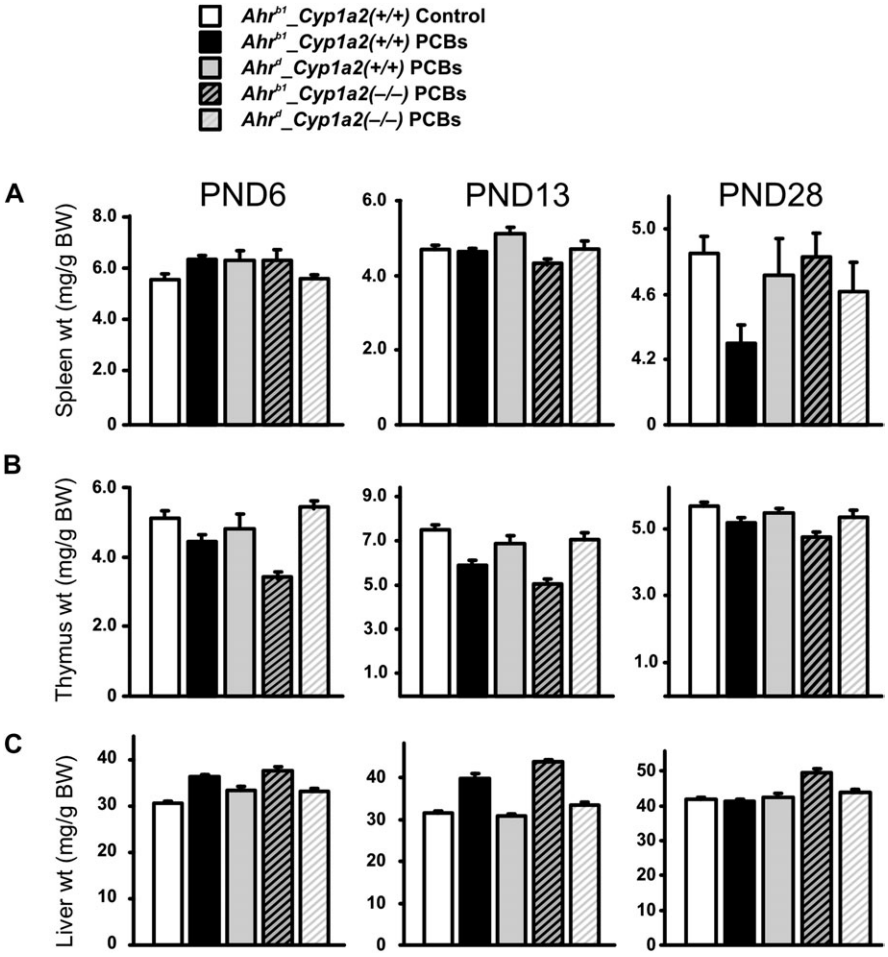

FIG. 6 Spleen, thymus, and liver weights depicted as milligrams per gram body weight (BW). Wet weights ($N \geq 10$ per group) were recorded at three postnatal time points. In this and subsequent panels, weights from PCB-treated animals of all four genotypes were compared with weights from corn oil–treated B6 controls at the same ages. Interindividual and group statistics are available upon request. (Top row) There were no significant differences in spleen weights at PND6. At PND13, spleen weights were significantly decreased in *Ahr^{b1}_Cyp1a2(−/−)* pups. At PND28, spleen weights were significantly decreased in *Ahr^{b1}_Cyp1a2(+/+)* pups. (Middle row) At PND6, there were significant decreases in thymus weights in *Ahr^{b1}*-containing mice. At PND13, thymus wet weights were significantly decreased in all genotypes, but the greatest decrease was seen in *Ahr^{b1}*-containing pups. At PND28, thymus wet weights were significantly decreased only in *Ahr^{b1}_Cyp1a2(+/+)* pups. (Bottom row) At PND6, there were significant increases in liver weight in all PCB-treated groups compared with controls. At PND13, liver weights were only increased in *Ahr^{b1}*-containing pups. At PND28, liver weights were increased significantly only in *Ahr^{b1}_Cyp1a2(−/−)* pups. Liver histology showed no differences in any of the genotypes throughout this time period (data not shown).

methylsulfonated metabolites can cross the placenta (Park *et al.*, 2009; Soechitram *et al.*, 2004), and some have reported half-lives nearly as long as the parent congeners (Hovander *et al.*, 2006; Linderholm *et al.*, 2010). The small amounts of tissue available in a rodent study precluded the analysis at this time, but the use of radiolabeled congeners offers an option for tracking such metabolites more effectively.

←
compared with *Ahr^{d}_Cyp1a2(+/+)* mothers and ~100-fold higher in *Ahr^{b1}_Cyp1a2(+/+)* pup liver compared with *Ahr^{d}_Cyp1a2(+/+)* pups. (Third row) PND6. CYP1A1 induction was ~1000-fold higher in *Ahr^{b1}*-containing maternal and pup liver compared with *Ahr^{d}*-containing mothers and pups. CYP1A2 mRNA levels were approximately eightfold higher in *Ahr^{b1}_Cyp1a2(+/+)* maternal liver compared with *Ahr^{d}_Cyp1a2(+/+)* mothers and > 10-fold higher in *Ahr^{b1}_Cyp1a2(+/+)* pup liver compared with *Ahr^{d}_Cyp1a2(+/+)* pups. (Fourth row) PND13. CYP1A1 induction was significantly higher in *Ahr^{b1}*-containing maternal and pup liver compared with *Ahr^{d}*-containing mothers and pups. CYP1A2 mRNA levels were approximately sixfold higher in *Ahr^{b1}_Cyp1a2(+/+)* maternal liver compared with *Ahr^{d}_Cyp1a2(+/+)* mothers and > 15-fold higher in *Ahr^{b1}_Cyp1a2(+/+)* pup liver compared with *Ahr^{d}_Cyp1a2(+/+)* pups. (Bottom row) PND28. CYP1A1 induction was significantly higher in *Ahr^{b1}_Cyp1a2(−/−)* maternal liver compared with mothers from the other three genotypes. CYP1A1 induction was highest in *Ahr^{b1}*-containing pup liver compared with *Ahr^{b1}*-containing maternal liver and *Ahr^{d}*-containing pup liver. In pup brain, CYP1A1 was significantly induced in *Ahr^{b1}_Cyp1a2(−/−)* pups compared with pups from the other three genotypes. CYP1A2 mRNA was significantly higher in both *Ahr^{b1}_Cyp1a2(+/+)* and *Ahr^{d}_Cyp1a2(+/+)* pup liver. In this figure and the next, ''significantly'' denotes p values anywhere between < 0.05 and < 0.0001.

CYP1A1 mRNA showed an increased trend that was not statistically significant ($p > 0.05$), in *Ahr^{b1}_Cyp1a2(+/+)* pup brain at PND28, whereas CYP1A1 mRNA was still statistically significantly induced in *Ahr^{b1}_Cyp1a2(−/−)* pup brain at PND28 (Fig. 5E). This observation is consistent with hepatic CYP1A2 acting as a "sink" (Dragin *et al.*, 2006)—when maternal CYP1A2 is absent, more PCBs reach the offspring.

The Figure 5 data confirm that the effect of CYP1A induction by coplanar PCBs can be seen not only in maternal liver but also in embryonic, fetal, and neonatal liver, as well as in PND28 brain. In other words, we achieved our goal of the PCB mixture regimen having a significant effect on the maternal-fetal unit—including AHR activation in postnatal brain. These data give us encouragement to proceed with the behavioral studies (to be described elsewhere).

Interestingly, decreases in PND13 and PND28 spleen weight (Fig. 6A)—as well as PND6, PND13, and PND28 thymus weight (Fig. 6B)—are more closely related to the *Ahr* genotype than the presence or absence of CYP1A2. This finding is consistent with recent studies (Shi *et al.*, 2010) showing that intestinal inducible CYP1A1 is by far the most critical in detoxifying oral BaP—thereby preventing this PAH from distributing itself to distal tissues. Distal tissues, in this case, would include the intrauterine contents as well as pups receiving PCB-laced milk via lactation when the mother receives oral PAHs; distal tissues thus would also include pup spleen. Our present study indicates that this phenomenon extends from BaP to PCBs that are able to be metabolized by CYP1 enzymes; this finding further indicates that intestinal AHR affinity (and therefore inducible gut CYP1A1) is more crucial than the effect of maternal liver CYP1A2 acting as a sink to sequester AHR ligands such as coplanar PCBs. Unlike BaP, however, some more highly chlorinated PCBs (e.g., PCB 126) are not good CYP1 substrates, although they are excellent inducers of the CYP1 enzymes. Thus, an alternative explanation includes the possibility that persistent induction of CYP1 enzymes could lead to oxidative stress, thereby imposing more toxicity to the mice.

That pup splenic atrophy is more closely related to the *Ahr* genotype—than the presence or absence of CYP1A2—would further suggest that both *Cyp1a2(+/+)* and *Cyp1a2(−/−)* mothers received sufficient amounts of coplanar PCBs to elicit immunosuppression and activate the AHR receptor. Presumably, consistent with the (Dragin *et al.*, 2006) study, at some lower levels of coplanar PCBs being administered, we would be able to see an effect in pups of *Cyp1a2(−/−)* mothers but no effect in pups of *Cyp1a2(+/+)* mothers. But, perhaps not; a dose-response study would clarify this question.

The liver weight to total body weight ratio was dramatically increased—a sign of chronic AHR activation—in all four PCB-treated genotypes at PND6 compared with controls receiving no PCBs (Fig. 6C). The liver weight to total body weight ratio was significantly increased in the two *Ahr^{b1}*-containing mouse lines at PND13 but only in *Ahr^{b1}_Cyp1a2(−/−)* weanlings at PND28. Intriguingly, this is the mouse line that we had predicted would be most vulnerable to the PCBs' regimen (Table 2), and this is the same mouse line that had the highest amounts of coplanar PCB 126 and PCB 169 in PND28 pup inguinal fat (Tables 13 and 14).

Finally, can we extrapolate our mouse data to human populations? One might query whether the combination—of amount of exposure to coplanar PCBs, > 60-fold variation in basal and inducible hepatic CYP1A2 levels, and > 12-fold differences in AHR affinity—might be relevant to human risk assessment of PCB-induced birth defects. The answer to this question is not yet proven, but the present study, especially combined with the previous study (Dragin *et al.*, 2006), provides the basis for speculation about an "at-risk" subset in human populations. For example, the genotype of the affected fetus need not necessarily carry a teratogenic risk; rather, instead, a susceptible maternal genotype might be more crucial to risk of birth defects.

Hence, the highest risk for PCB-induced birth defects is likely to be in one whose maternal liver has genetically very low CYP1A2 activity, combined with a fetus who expresses the highest AHR inducibility. This notion follows from the observation that, although fetal CYP1A2 does not contribute to PCB-induced teratogenesis because it is not expressed in the embryo or fetus (Nebert, 1989), fetal high-affinity AHR is probably essential for coplanar PCB-induced toxicity and teratogenesis, just as it is for TCDD-mediated teratogenesis (Peters *et al.*, 1999; Thomae *et al.*, 2004).

It should be noted that, for human cohort studies, determination of the precise level of environmental PCB exposure would be expected to be a confounding factor in such genotype-phenotype association studies. In addition, to date, no DNA variant sites in or near either the human *CYP1A2* or the *AHR* gene have been shown unequivocally to reflect variations in the CYP1A2 or AHR phenotype (Jiang *et al.*, 2006; Nebert *et al.*, 2004).

FUNDING

National Institutes of Health Grants (R21 ES015335 to D.W.N., C.V.V., M.T.W.; T32 ES007051 to C.P.C.; P30 ES06096 to D.W.N.).

ACKNOWLEDGMENTS

We thank our colleagues for valuable discussions and help during the course of this work and careful readings of the

manuscript—especially Ying Chen (now at University of Colorado, Denver), Larry G. Hansen (University of Illinois, Professor Emeritus), and many colleagues including John Lipscomb at the U.S. Environmental Protection Agency and Stephen Winslow at Shaw Environmental (who allowed C.P.C. to use their equipment). Portions of this work were presented at the Society of Toxicology 46th Annual Meeting in March 2007, Charlotte, NC, and the Teratology Society 49th Annual Meeting in June 2009, Puerto Rico.

REFERENCES

Agency for Toxic Substances and Disease Registry (ATSDR). (2001). *ToxFaq: Polychlorinated Biphenyls*. U.S. Department of Health and Human Services, Public Health Service. Atlanta, GA. [Pamphlet].

Battershill, J. M. (1994). Review of the safety assessment of polychlorinated biphenyls (PCBs) with particular reference to reproductive toxicity. *Hum. Exp. Toxicol.* **13,** 581–597.

Bhavsar, S. P., Hayton, A., Reiner, E. J., and Jackson, D. A. (2007). Estimating dioxin-like polychlorinated biphenyl toxic equivalents from total polychlorinated biphenyl measurements in fish. *Environ. Toxicol. Chem.* **26,** 1622–1628.

Chishti, M. A., Fisher, J. P., and Seegal, R. F. (1996). Aroclors 1254 and 1260 reduce dopamine concentrations in rat striatal slices. *Neurotoxicology* **17,** 653–660.

Clancy, B., Kersh, B., Hyde, J., Darlington, R. B., Anand, K. J., and Finlay, B. L. (2007). Web-based method for translating neurodevelopment from laboratory species to humans. *Neuroinformatics* **5,** 79–94.

Costabeber, I., Dos Santos, J. S., Xavier, A. A., Weber, J., Leaes, F. L., Junior, S. B., and Emanuelli, T. (2006). Levels of polychlorinated biphenyls (PCBs) in meat and meat products from the state of Rio Grande do Sul, Brazil. *Food Chem. Toxicol.* **44,** 1–7.

Curran, C. P., Miller, K. A., Dalton, T. P., Vorhees, C. V., Miller, M. L., Shertzer, H. G., and Nebert, D. W. (2006). Genetic differences in lethality of newborn mice treated in utero with coplanar versus non-coplanar hexabromobiphenyl. *Toxicol. Sci.* **89,** 454–464.

Dewailly, E., Mulvad, G., Pedersen, H. S., Ayotte, P., Demers, A., Weber, J. P., and Hansen, J. C. (1999). Concentration of organochlorines in human brain, liver, and adipose tissue autopsy samples from Greenland. *Environ. Health Perspect.* **107,** 823–828.

Dragin, N., Dalton, T. P., Miller, M. L., Shertzer, H. G., and Nebert, D. W. (2006). For dioxin-induced birth defects, mouse or human CYP1A2 in maternal liver protects whereas mouse CYP1A1 and CYP1B1 are inconsequential. *J. Biol. Chem.* **281,** 18591–18600.

Gauger, K. J., Kato, Y., Haraguchi, K., Lehmler, H. J., Robertson, L. W., Bansal, R., and Zoeller, R. T. (2004). Polychlorinated biphenyls (PCBs) exert thyroid hormone-like effects in the fetal rat brain but do not bind to thyroid hormone receptors. *Environ. Health Perspect.* **112,** 516–523.

Guo, Y. L., Yu, M. L., Hsu, C. C., and Rogan, W. J. (1999). Chloracne, goiter, arthritis, and anemia after polychlorinated biphenyl poisoning: 14-year follow-up of the Taiwan Yucheng cohort. *Environ. Health Perspect.* **107,** 715–719.

Gustavsson, P., and Hogstedt, C. (1997). A cohort study of Swedish capacitor manufacturing workers exposed to polychlorinated biphenyls (PCBs). *Am. J. Ind. Med.* **32,** 234–239.

Hakk, H., Diliberto, J. J., and Birnbaum, L. S. (2009). The effect of dose on 2,3,7,8-TCDD tissue distribution, metabolism and elimination in *Cyp1a2(-/-)* knockout and C57BL/6N parental strains of mice. *Toxicol. Appl. Pharmacol.* **241,** 119–126.

Hovander, L., Linderholm, L., Athanasiadou, M., Athanassiadis, I., Bignert, A., Fangstrom, B., Kocan, A., Petrik, J., Trnovec, T., and Bergman, A. (2006). Levels of PCBs and their metabolites in the serum of residents of a highly contaminated area in eastern Slovakia. *Environ. Sci. Technol.* **40,** 3696–3703.

Imbeault, P., Chevrier, J., Dewailly, E., Ayotte, P., Despres, J. P., Mauriege, P., and Tremblay, A. (2002). Increase in plasma pollutant levels in response to weight loss is associated with the reduction of fasting insulin levels in men but not in women. *Metabolism* **51,** 482–486.

Imsilp, K., Wiedenmann, L., Bordson, G. O., Morrow, C. K., Cope, R., and Hansen, L. G. (2005). Time- and tissue-dependent polychlorinated biphenyl residues in *hairless* mice after exposure to polychlorinated biphenyl-contaminated soil. *Arch. Environ. Contam. Toxicol.* **49,** 105–118.

Jiang, Z., Dragin, N., Jorge-Nebert, L. F., Martin, M. V., Guengerich, F. P., Aklillu, E., Ingelman-Sundberg, M., Hammons, G. J., Lyn-Cook, B. D., Kadlubar, F. F., *et al.* (2006). Search for an association between the human *CYP1A2* genotype and CYP1A2 metabolic phenotype. *Pharmacogenet. Genomics* **16,** 359–367.

Kang, J. H., Jeong, W., Park, Y., Lee, S. Y., Chung, M. W., Lim, H. K., Park, I. S., Choi, K. H., Chung, S. Y., Kim, D. S., *et al.* (2002). Aroclor 1254-induced cytotoxicity in catecholaminergic 'CATH.a' cells related to the inhibition of NO production. *Toxicology* **177,** 157–166.

Karlen, Y., McNair, A., Perseguers, S., Mazza, C., and Mermod, N. (2007). Statistical significance of quantitative PCR. *BMC Bioinformatics* **8,** 131.

Kimura-Kuroda, J., Nagata, I., and Kuroda, Y. (2005). Hydroxylated metabolites of polychlorinated biphenyls inhibit thyroid-hormone-dependent extension of cerebellar Purkinje cell dendrites. *Brain Res. Dev. Brain Res.* **154,** 259–263.

Liang, H. C., Li, H., McKinnon, R. A., Duffy, J. J., Potter, S. S., Puga, A., and Nebert, D. W. (1996). *Cyp1a2(-/-)* null mutant mice develop normally but show deficient drug metabolism. *Proc. Natl. Acad. Sci. U.S.A.* **93,** 1671–1676.

Linderholm, L., Biague, A., Mansson, F., Norrgren, H., Bergman, A., and Jakobsson, K. (2010). Human exposure to persistent organic pollutants in West Africa—a temporal trend study from Guinea-Bissau. *Environ. Int.* **36,** 675–682.

Masuda, Y. (2001). Fate of PCDF/PCB congeners and change of clinical symptoms in patients with Yusho PCB poisoning for 30 years. *Chemosphere* **43,** 925–930.

Meerts, I. A., Lilienthal, H., Hoving, S., van den Berg, J. H., Weijers, B. M., Bergman, A., Koeman, J. H., and Brouwer, A. (2004). Developmental exposure to 4-hydroxy-2,3,3′,4′,5-pentachlorobiphenyl (4-OH-CB107): long-term effects on brain development, behavior, and brain stem auditory evoked potentials in rats. *Toxicol. Sci.* **82,** 207–218.

Nebert, D. W. (1989). The *Ah* locus: genetic differences in toxicity, cancer, mutation, and birth defects. *Crit. Rev. Toxicol.* **20,** 153–174.

Nebert, D. W., Dalton, T. P., Okey, A. B., and Gonzalez, F. J. (2004). Role of aryl hydrocarbon receptor-mediated induction of the CYP1 enzymes in environmental toxicity and cancer. *J. Biol. Chem.* **279,** 23847–23850.

Nebert, D. W., Goujon, F. M., and Gielen, J. E. (1972). Aryl hydrocarbon hydroxylase induction by polycyclic hydrocarbons: autosomal dominant trait in the mouse. *Nat. New Biol.* **236,** 107–110.

Nebert, D. W., Roe, A. L., Dieter, M. Z., Solis, W. A., Yang, Y., and Dalton, T. P. (2000). Role of the aromatic hydrocarbon receptor and [*Ah*] gene battery in the oxidative stress response, cell cycle control, and apoptosis. *Biochem. Pharmacol.* **59,** 65–85.

Negri, E., Bosetti, C., Fattore, E., and La, V. C. (2003). Environmental exposure to polychlorinated biphenyls (PCBs) and breast cancer:

a systematic review of the epidemiological evidence. *Eur. J. Cancer Prev.* **12,** 509–516.

Nelson, D. R., Zeldin, D. C., Hoffman, S. M., Maltais, L. J., Wain, H. M., and Nebert, D. W. (2004). Comparison of cytochrome P450 (*CYP*) genes from the mouse and human genomes, including nomenclature recommendations for genes, pseudogenes and alternative-splice variants. *Pharmacogenetics* **14,** 1–18.

Oberg, M., Sjodin, A., Casabona, H., Nordgren, I., Klasson-Wehler, E., and Hakansson, H. (2002). Tissue distribution and half-lives of individual polychlorinated biphenyls and serum levels of 4-hydroxy-2,3,3′,4′,5-pentachlorobiphenyl in the rat. *Toxicol. Sci.* **70,** 171–182.

Park, H. Y., Park, J. S., Sovcikova, E., Kocan, A., Linderholm, L., Bergman, A., Trnovec, T., and Hertz-Picciotto, I. (2009). Exposure to hydroxylated polychlorinated biphenyls (OH-PCBs) in the prenatal period and subsequent neurodevelopment in eastern Slovakia. *Environ. Health Perspect.* **117,** 1600–1606.

Peters, J. M., Narotsky, M. G., Elizondo, G., Fernandez-Salguero, P. M., Gonzalez, F. J., and Abbott, B. D. (1999). Amelioration of TCDD-induced teratogenesis in aryl hydrocarbon receptor *Ahr(-/-)* null mice. *Toxicol. Sci.* **47,** 86–92.

Petrik, J., Drobna, B., Pavuk, M., Jursa, S., Wimmerova, S., and Chovancova, J. (2006). Serum PCBs and organochlorine pesticides in Slovakia: age, gender, and residence as determinants of organochlorine concentrations. *Chemosphere* **65,** 410–418.

Poland, A., and Glover, E. (1977). Chlorinated biphenyl induction of aryl hydrocarbon hydroxylase activity: a study of the structure-activity relationship. *Mol. Pharmacol.* **13,** 924–938.

Poland, A., Palen, D., and Glover, E. (1994). Analysis of the four alleles of the mouse aryl hydrocarbon receptor. *Mol. Pharmacol.* **46,** 915–921.

Poland, A. P., Glover, E., Robinson, J. R., and Nebert, D. W. (1974). Genetic expression of aryl hydrocarbon hydroxylase activity. Induction of monooxygenase activities and cytochrome P_1-450 formation by 2,3,7,8-tetrachlorodibenzo-*p*-dioxin in mice genetically "nonresponsive" to other aromatic hydrocarbons. *J. Biol. Chem.* **249,** 5599–5606.

Sartor, M. A., Schnekenburger, M., Marlowe, J. L., Reichard, J. F., Wang, Y., Fan, Y., Ma, C., Karyala, S., Halbleib, D., Liu, X., *et al.* (2009). Genomewide analysis of aryl hydrocarbon receptor binding targets reveals an extensive array of gene clusters that control morphogenetic and developmental programs. *Environ. Health Perspect.* **117,** 1139–1146.

Schantz, S. L., Sweeney, A. M., Gardiner, J. C., Humphrey, H. E., McCaffrey, R. J., Gasior, D. M., Srikanth, K. R., and Budd, M. L. (1996). Neuropsychological assessment of an aging population of Great Lakes fisheaters. *Toxicol. Ind. Health* **12,** 403–417.

Seegal, R. F., Brosch, K. O., and Okoniewski, R. J. (1997). Effects of in utero and lactational exposure of the laboratory rat to 2,4,2′,4′- and 3,4,3′,4′-tetrachlorobiphenyl on dopamine function. *Toxicol. Appl. Pharmacol.* **146,** 95–103.

Selgrade, M. K. (2007). Immunotoxicity: the risk is real. *Toxicol. Sci.* **100,** 328–332.

Shi, Z., Dragin, N., Galvez-Peralta, M., Jorge-Nebert, L. F., Miller, M. L., Wang, B., and Nebert, D. W. (2010). Organ-specific roles of CYP1A1 during detoxication of dietary benzo[*a*]pyrene. *Mol. Pharmacol.* **78,** 46–57.

Simon, T., Britt, J. K., and James, R. C. (2007). Development of a neurotoxic equivalence scheme of relative potency for assessing the risk of PCB mixtures. *Regul. Toxicol. Pharmacol.* **48,** 148–170.

Soechitram, S. D., Athanasiadou, M., Hovander, L., Bergman, A., and Sauer, P. J. (2004). Fetal exposure to PCBs and their hydroxylated metabolites in a Dutch cohort. *Environ. Health Perspect.* **112,** 1208–1212.

Takser, L., Mergler, D., Baldwin, M., de, G. S., Smargiassi, A., and Lafond, J. (2005). Thyroid hormones in pregnancy in relation to environmental exposure to organochlorine compounds and mercury. *Environ. Health Perspect.* **113,** 1039–1045.

Tan, S. W., and Zoeller, R. T. (2007). Integrating basic research on thyroid hormone action into screening and testing programs for thyroid disruptors. *Crit. Rev. Toxicol.* **37,** 5–10.

Thomae, T. L., Glover, E., and Bradfield, C. A. (2004). A maternal *Ahr(-/-)* null genotype sensitizes embryos to chemical teratogenesis. *J. Biol. Chem.* **279,** 30189–30194.

Ulbrich, B., and Stahlmann, R. (2004). Developmental toxicity of polychlorinated biphenyls (PCBs): a systematic review of experimental data. *Arch. Toxicol.* **78,** 252–268.

Uno, S., Dalton, T. P., Derkenne, S., Curran, C. P., Miller, M. L., Shertzer, H. G., and Nebert, D. W. (2004). Oral exposure to benzo[*a*]pyrene in the mouse: detoxication by inducible cytochrome P450 is more important than metabolic activation. *Mol. Pharmacol.* **65,** 1225–1237.

Uno, S., Dragin, N., Miller, M. L., Dalton, T. P., Gonzalez, F. J., and Nebert, D. W. (2008). Basal and inducible CYP1 mRNA quantitation and protein localization throughout mouse gastrointestinal tract. *Free Radic. Biol. Med.* **44,** 570–583.

Van Birgelen, A. P., Smit, E. A., Kampen, I. M., Groeneveld, C. N., Fase, K. M., Van der, K. J., Poiger, H., Van den, B. M., Koeman, J. H., and Brouwer, A. (1995). Subchronic effects of 2,3,7,8-TCDD or PCBs on thyroid hormone metabolism: use in risk assessment. *Eur. J. Pharmacol.* **293,** 77–85.

Van den Berg, M., Birnbaum, L. S., Denison, M., De, V. M., Farland, W., Feeley, M., Fiedler, H., Hakansson, H., Hanberg, A., Haws, L., *et al.* (2006). The 2005 World Health Organization reevaluation of human and mammalian toxic equivalency factors for dioxins and dioxin-like compounds. *Toxicol. Sci.* **93,** 223–241.

Wang, S. L., Su, P. H., Jong, S. B., Guo, Y. L., Chou, W. L., and Papke, O. (2005). In utero exposure to dioxins and polychlorinated biphenyls and its relationship to thyroid function and growth hormone in newborns. *Environ. Health Perspect.* **113,** 1645–1650.

World Health Organization (WHO). (1996). *Levels of PCBs, PCDDs and PCDFs in human milk. Second round of WHO-coordinated exposure study. 6-1-1996.* World Health Organization, European Centre for Environment and Health, Copenhagen, Denmark. [Pamphlet].